Argonne
NATIONAL LABORATORY

CFD Analysis for the Applicability of the Natural Convection Shutdown Heat Removal Test Facility (NSTF) for the Simulation of the VHTR RCCS

Topical Report

Nuclear Engineering Division

CFD Analysis for the Applicability of the Natural Convection Shutdown Heat Removal Test Facility (NSTF) for the Simulation of the VHTR RCCS

Topical Report

by
C.P. Tzanos
Nuclear Engineering Division, Argonne National Laboratory

September 2005

Table of Contents

List of Figures

3

List of Tables

1.0. INTRODUCTION

The Very High Temperature gas cooled reactor (VHTR) is one of the GEN IV reactor concepts that have been proposed for thermochemical hydrogen production and other process-heat applications like coal gasification. The United States Department of Energy has selected the VHTR for further research and development, aiming to demonstrate emissions-free electricity and hydrogen production at a future time.

One of the major safety advantages of the VHTR is the potential for passive decay heat removal by natural circulation of air in a Reactor Cavity Cooling System (RCCS). The air-side of the RCCS is very similar to the Reactor Vessel Auxiliary Cooling System (RVACS) that has been proposed for the PRISM reactor design. The design and safety analysis of the RVACS have been based on extensive analytical and experimental work performed at ANL. The Natural Convection Shutdown Heat Removal Test Facility (NSTF) at ANL that simulates at full scale the air-side of the RVACS was built to provide experimental support for the design and analysis of the PRISM RVACS system. The objective of this work is to demonstrate that the NSTF facility can be used to generate RCCS experimental data: to validate CFD and systems codes for the analysis of the RCCS; and to support the design and safety analysis of the RCCS.

At this time no reference design is available for the NGNP. The General Atomics (GA) gas turbine – modular helium reactor (GT-MHR) has been used in many analyses as a starting reference design [1]. In the GT-MHR the reactor outlet temperature is 850 °C, while the target outlet reactor temperature in VHTR is 1000 °C. VHTR scoping studies with a reactor outlet temperature of 1000 °C have been performed at GA and INEL. Although the reactor outlet temperature in the VHTR is significantly higher than in the GT-MHR, the peak temperature in the reactor vessel (which is the heat source for the RCCS) is not drastically different. In this work, analyses have been performed using reactor vessel temperatures from the GT-MHR design, and the VHTR scoping studies.

To demonstrate the applicability of the NSTF facility for full scale simulation of the RCCS the following approach was used. CFD analyses were performed of the RCCS and of its simulation at NSTF to demonstrate that: all significant fluid flow and heat transfer phenomena in the RCCS can be simulated at NSTF; and RCCS simulations at NSTF can cover the whole range of variation of the parameters describing these important phenomena in the RCCS.

In CFD analyses, the simulation of turbulence is one of the most significant challenges. Direct Numerical Simulation (DNS) and Large Eddy Simulation (LES) of turbulence in large scale systems require excessive computational resources. The use of the Low-Re number k-ε model, which resolves the boundary layer, is computationally expensive in studies where many simulations have to be performed. In Ref. 2 it was shown that in the RCCS, heat transfer coefficient predictions of the high-Re number k-ε model are closer to those of the low-Re number model than those of heat transfer correlations. In this work, the standard high-Re number k-ε was used to simulate turbulence, and all analyses were performed with the CFD code STAR-CD.

2.0. MODEL DESCRIPTION

For the purpose of this project two STAR-CD models were constructed. One model simulated the RCCS and its environs within the plant. The second model simulated the RCCS in the environs of the NSTF. In addition, a separate effects type model was developed to simulate the pressure drop of the RCCS inclusive of the air stack.

2.1 CFD Model of the RCCS in the Plant Geometry

The RCCS provides decay heat removal during long-term loss of forced convection transients. Figure 1 is a simplified schematic of the GT-MHR RCCS. It consists of 292 rectangular ducts (tubes) arranged around the reactor vessel. Each tube is a standard structural steel tube having dimensions of 5.05 cm x 25.4 cm with a wall thickness of 0.47625 cm.

Air at 43°C, driven by natural convection, enters an inlet plenum above the downcomer, then flows through the downcomer (which is attached to the containment wall) to the bottom of the reactor compartment, where it is distributed to the RCCS tubes. The hot air leaving the tubes is collected in a plenum, and from there through chimneys is discharged to the atmosphere. Heat is transferred from the reactor vessel to the tubes mainly by radiation, and by convection. Figure 1, illustrates the radiation paths between the reactor vessel, the tubes, the downcomer walls, and the downcomer wall facing the tubes. This wall has a highly reflective surface, and is backed by a 7.62 cm of microtherm insulation. It should be noted that radiation between the tube walls is also significant and has been modeled in the analyses of this report..

To simulate the VHTR RCCS, the reasonable assumption is made that its tube design will not be significantly different than that of the GT-MHR. Even with this assumption information is needed at least for the pressure drops in the RCCS sections before and after the tube heated section. At this time such information is not available in the literature even for the GT-MHR. An approximate estimate of these pressure drops can be obtained as discussed in section 2.3 from the RCCS performance data (heat removed and air flow rate) of the GT-MHR at steady state.

Because the performance of the GT-MHR RCCS tubes is nearly identical, for the purposes of this analysis the assumption was made that the performance of all tubes is the same, and only one-half of a tube plus one-half of the gap between the tubes was modeled. Also, because no information is available for the design of the downcomer, of inlet and outlet plena and the discharge chimneys, they were not directly simulated. The pressure drop in these sections was accounted as discussed in section 2.3. As shown in Fig. 2, the simulation included the reactor vessel wall, the air in the reactor cavity, the cavity top and bottom walls, one-half of an RCCS tube, one-half of the gap between the tubes, and the insulation in front of the downcomer.

2.2 CFD Model of the RCCS at NSTF

The NSTF facility at ANL was built and used to simulate a section of the RVACS air-flow path of the PRISM ALMR design. This section is a duct formed by the reactor guard vessel (heated wall) and the outer duct wall surrounding the guard vessel. The facility   consists of a structural module, electric heaters, instrumentation, insulation, and a computerized control and data acquisition system. It operates in one of the following thermal modes: (1) constant (uniform) guard vessel wall temperature to 950 K (677°C); (2) constant (uniform) heat flux to 21.5 kw/; and stepwise variation of either of the previous modes singly, or in combination.

The basic assembly configuration is shown in Fig. 3. It consists of an inlet section followed by a heated zone and an unheated stack or chimney. All sections, with the exception of the inlet, are thermally insulated to reduce parasitic heat losses to a minimum. The heated channel has a cross section of 1.32 m (52 in.) x 0.304 m (12 in.), and a height of 6.7m. The 0.304 gap can be extended up to 0.456 m (18 in.), or reduced to any desired value. Construction details of the test section are shown in Fig. 4. The surfaces that simulate the guard vessel wall (heated wall) and the outer duct wall are smooth carbon steel plates 2.54 cm (1 in.) thick. Within the heated zone,

fins or ribs could be installed on the inner walls of the air channel to enhance turbulence and heat transfer.

Above the heated zone the flow channel expands to a cross section of 1.32 m (52 in.) x 0.456 m (18 in.) and two flow paths are provided. The main path for the experiments is upward through an "S" curve and then vertically through the building roof. This provides a stack for natural convection nearly 15.2 m (50 ft) in vertical length. The top of the stack is 6.1 m (20 ft) above the roof. The second flow path contains a fan with a variable motor speed and a damper. This feature is provided for forced convection tests, when the system is at very low temperature and a controlled air flow rate is desired. Heat input to the guard vessel is provided by an assembly of electrical heaters that are fastened to a 0.635 cm (0.25 in.) stainless steel plate. Heat is transferred through the plate and then conducted across a small gap to the guard vessel surface. Power to the heaters is computer controlled based on signals from system thermocouples.

The data acquisition system (DAS) was capable of sampling 300 channels, most of which are dedicated to thermocouples located in the heated zone. The DAS stores all its data on disk and selected channels may also be displayed on CTRs and hardcopy.   The computer was programmed to use on-line data to compute system parameters for real-time display and hardcopy. The heater power and control system design and the data acquisition system are shown in Fig. 5. In an NSTF facility adapted for RCCS experiments, the DAS system will be completely renovated to satisfy the RCCS needs.

Instrumentation is provided to measure local surface temperatures, local bulk air temperatures, local and bulk air velocities, air volumetric and mass flow rates, the total normal radiative heat flux, and electrical power to the heaters. The instrumentation consists of thermocouples, Pitot-static traversing probes, a Pitot-static air flow "rake," differential pressure transducers, radiation flux transducers, an anemometer and air pressure and humidity gages.   Data from these measurements are used to evaluate the heat removal performance for particular configurations and testing conditions. The primary measurement objective was to determine the local and bulk heat flux transport rates and associated heat transfer coefficients. In an NSTF facility adapted for RCCS experiments, the instrumentation will be augmented to satisfy the RCCS needs.

A CFD model was developed to simulate the thermal-hydraulic performance of the NSTF facility. In this model the assumptions were made that each tube behaves as if there was an infinite number of tubes, and the inlet section of the tubes was properly rounded to reduce the inlet pressure loss coefficient to a value of 0.05. The model (Fig. 6) includes the reactor vessel wall, one-half of one tube, one-half of the gap between tubes (assumption of symmetry), a 2.54 carbon steel plate, and a 15.24 insulation plate (hydrous calcium silicate, Johns Manville Thermo-12 insulation). The gap between the tube and the reactor vessel, as well as the gap between the tube and the carbon steel plate is 10.1 cm. In the flow direction, only the heated section was modeled. Pressure drops for the sections of the NSTF flow path that were not directly modeled were accounted as discussed in section 2.3.

Figure 7 shows in scale a cross section of the NSTF flow path and two RCCS tubes inside this flow path. Actually, up to twelve RCCS tubes (tubes plus gap region between tubes) can be placed inside the NSTF flow path to experimentally study the thermal performance of the RCCS. In this arrangement, the heated wall of the facility channel will simulate the wall of the reactor vessel, which is the heat source of the RCCS, and the other channel wall will simulate the insulation of the inner surface (reactor cavity side) of the RCCS downcomer. Measurements will be performed in the central tube, and possibly in some adjacent tubes, while the other tubes will provide the proper radiative surfaces for the simulation of the actual RCCS-tube configuration.

In this arrangement, the cross section of the RCCS tubes is simulated at full-scale. In the GT-MHR design of GA the distance between the outer surface of the reactor vessel and the front side of the RCCS tubes is 0.77 m. In the NSTF facility this distance would be of the order of 0.1 m. This will have an effect on the view factors between the reactor vessel and the RCCS tubes. As discussed in Section 4.1, this effect is small. The outer wall of the air flow channel in the NSTF facility was originally intended to simulate the outer duct wall of the RVACS, which was made of the same material as the guard vessel. In the RCCS, this wall simulates the outer surface of the insulation of the RCCS downcomer, which does not have the same emissivity as the reactor vessel wall. As shown in Section 4.1, the effect of this difference, is not significant.

2.3 Pressure Drop Model (including stack)

The static pressure, p_{in}, at the inlet of the RCCS is

$$p_{in} = p_{out} + \rho_o g(H_h + H_s) \tag{1}$$

where

p_{out} = static pressure at the RCCS stack outlet
H_h = length of the heated section
H_s = length of the stack

The pressure at the inlet is also

$$p_{in} = p_{out} + \int_0^{H_h} \rho g dh + \rho_s g H_s + \text{total pressure losses} \tag{2}$$

The total pressure losses, Δp_{tot}, are

$$\Delta p_{tot} = \Delta p_f + \Delta p_a + \Delta p_{other} \tag{3}$$

where Δp_f and Δp_a are the frictional and acceleration pressure drops in the heated section and Δp_{other} are all other pressure drops. From Eqs (1) and (2)

$$\rho_o g \left(H_h + H_s\right) - \int_0^{H_h} \rho g dh - \rho_s g H_s = \Delta p_f + \Delta p_a + \Delta p_{other}$$

or

$$\int_0^{H_h} \left(\rho_o - \rho\right) g dh + g H_s \left(\rho_o - \rho_s\right) = \Delta p_f + \Delta p_a + \Delta p_{other}$$

or

$$\Delta p_{other} = \int_0^{H_h} \left(\rho_o - \rho\right) g dh + g H_s \left(\rho_o - \rho_s\right) - \Delta p_f - \Delta p_a \tag{4}$$

For the GT-MHR RCCS at steady state, Ref 1 gives a heat removal rate of 3.3 MW and a flow rate of 14.3 kg/s. STAR-CD simulations of the RCCS show that the bulk air temperature variation along the heated section of the tube is nearly linear. With this variation

9

$$\int_0^{H_h} (\rho_o - \rho) g\,dh + gH_s (\rho_o - \rho_s) = \rho_o g \left\{ \left[1 - \frac{\ln(T_e/T_o)}{T_e/T_o - 1} \right] H_h + \left(1 - \frac{\rho_s}{\rho_o} \right) H_s \right\} \tag{5}$$

$$\Delta\rho_f = \frac{2f_h W^2}{D_h \rho_0 T_0 A_h^2} \int_0^{H_h} \left(T_0 + \frac{T_e - T_0}{H_h} h \right) dh = \frac{f_h W^2}{D_h \rho_0 A_h^2} \left[H_h \left(1 + \frac{T_e}{T_0} \right) \right] \tag{6}$$

where

W	=	air mass flow rate
D_h	=	hydraulic diameter of the heated section
A_h	=	flow area at heated section
f_s	=	friction factor
ρ	=	air density
ρ_o	=	air density at the inlet of the heated section
ρ_s	=	air density at the exit of the heated section
T_o	=	air temperature at the inlet of the heated section
T_e	=	air temperature at the exit of the heated section

The acceleration pressure drop is

$$\Delta p_a = \frac{W^2}{A_h^2} \left(\frac{1}{\rho_s} - \frac{1}{\rho_0} \right) \tag{7}$$

The friction coefficient f_h can be computed from

$$f_h = 0.0791 \, \text{Re}_h^{-0.25} \tag{8}$$

For a rectangular duct Petukhov [3] gives the correlation

$$f_h = 0.25 \left[1.82 \log \left(\text{Re}/8 \right) \right]^{-2} \tag{9}$$

For the RCCS duct the friction factor values given by Eqs (8) and (9) differ by 1.7 %. Thus, either of them can be used. A small computer program was written that computes Δp_{other} from Eqs (4), (5), (6), (7) and (8).

The pressure drop Δp_{other} can be approximated by

$$\Delta p_{other} = K_L \frac{W^2}{2\rho_0 A_h^2} \tag{10}$$

to compute a pressure loss coefficient K_L. This pressure loss coefficient is used in STAR-CD to simulate the RCCS for conditions other than the GT-MHR steady state, where the RCCS flow rate is given in Ref. 1.

In STAR-CD, to account for pressure losses represented by a pressure loss coefficient the porous media model can be used. In this model, the pressure loss along a length L is computed from

$$\Delta p = KuL \tag{11}$$

where the resistance K is given as

$$K = \alpha|u| + \beta \tag{12}$$

From Eqs (10) and (11)

$$K = \frac{1}{2L} K_L \frac{\rho^2}{\rho_o} u \tag{13}$$

where ρ and u are the density and velocity at the location of the porous medium. From equations (12) and (13)

$$\alpha = \frac{1}{2L} K_L \frac{\rho^2}{\rho_0} \tag{14}$$

and β is set to a small number (here $\beta = 0.1$).

3.0   PLANT RCCS PERFORMANCE

Reference 1 (GT-MHR Conceptual Design Description Report) provides the following information on the steady state performance of the RCCS:

Heat loss to RCCS, kW	3300
Inside reactor vessel temperature, °C	485
Maximum outside reactor vessel temperature, °C	474
Air inlet temperature, °C	43
Air outlet temperature, °C	274
Airflow, kg/sec	14.3

In Reference 4 peak reactor vessel temperatures of 480 °C, 497 °C, and 490 °C are given for steady state conditions, High Pressure Conduction Cooldown (HPCC), and Low Pressure Conduction Cooldown (LPCC) transient conditions, respectively, for the GT-MHR design. Because these reactor vessel temperatures are not drastically different, RCCS simulations were performed for an outside reactor vessel temperature of 480 °C.

At this time a reference NGNP design is not available. INEEL has performed a number of scoping calculations for an NGNP design with a core coolant inlet temperature of 490 °C, a core coolant outlet temperature of 1000 °C, and a 10% core bypass flow (Ref. 5). Peak vessel temperatures varying from 509 to 563 °C were computed for different reactor power levels and

core block-heights, under the constraint that the peak fuel temperature does not exceed 1600 °C. Similar scoping analyses by GA (Ref. 5) report peak vessel temperatures that do not exceed 533 °C. These peak vessel temperatures are not drastically higher than those of the GT-MHR.

In October 2004, INEEL provided to ANL plant information for an NGNP design having also a core outlet temperature of 1000 C. For this design RELAP HPCC and LPCC transient analyses were performed by ANL. The LPCC transient gave a higher peak fuel temperature, which is reached at 76.7 hr from transient initiation. RELAP predicted at 76.7 hr an outside reactor vessel peak temperature of 467 °C at 6 m from the bottom of the lower reflector and an RCCS flow rate of 13.32 kg/s.

CFD RCCS simulations were performed:

(a) For a uniform reactor vessel temperature of 480 °C, and an RCCS flow rate of 14.3 kg/s (GT- MHR steady state).
(b) For a uniform reactor vessel temperature of 560 °C.
(c) For a peak reactor vessel temperature of 560 °C
(d) For the reactor vessel temperature distribution and RCCS flow rate at 76.7 hr determined by the ANL RELAP analysis of the LPCC transient mentioned above.

3.1 Uniform Reactor Vessel Temperature of 480 °C (GT-MHR Steady State)

In this simulation the following boundary conditions were used: a temperature of 480 °C for the outer reactor vessel surface; a temperature of 43 °C at the outer surface of the insulation; a tube flow rate as provided in Ref. 1; and an air inlet temperature of 43 °C (Ref. 1).

Figure 8 shows the temperature distribution on a tube cross-section at 14.9 m from the tube inlet (tube outlet at 15.6 m). This distribution is very asymmetric and reaches a minimum around the center of the back half of the tube. The maximum to minimum difference is 137 °C. The temperature distribution on the front and back walls of the tube are nearly uniform, but there is a large temperature variation from front to back on the side wall of the tube. This variation is about 111 °C.

Figure 9 shows the heat transfer coefficient along the axis of the front, side and back tube walls as predicted by the high-Re number model of turbulence. These heat transfer coefficients are based on the fluid temperature of the cells next to the wall. As it will be shown later these coefficients are more meaningful than coefficients based on the bulk air temperature. Figure 10) shows the variation of the heat transfer coefficient around the tube at 14.9 m from the tube inlet. These figures show a variation of the heat transfer coefficient around the tube as well as along the tube. The heat transfer coefficient is significantly higher on the side wall, and at any cross-section of this wall the variation of the heat transfer coefficient from the front to the back end of this wall is significantly higher than in the other two tube walls (front and back).

Figure 11 shows the variation of the heat flux around a tube at heights of 1.0m, 7.8 m, and 14.9 m. At 1.0m the heat flux peaks on the front wall, then at higher locations the peak moves to the side-wall, and moves from the front section towards the back section of this wall as we move higher from the bottom to the top of the tube.

Figure 12 shows the Nusselt number along the axis of the three tube walls. Figures 13 and 14 show the variation of the Grashof, Raleigh and Buoyancy (Bo) [6] numbers along the front side of the RCCS tube. More specifically these numbers were computed from the expressions:

$$Gr_L = \frac{\rho^2 g \beta (T_w - T_b) L^3}{\mu^2}$$

$$Ra_L = \text{Rayleigh number} = Gr_L \Pr$$

where

$$\Pr = \frac{\mu C_p}{k}$$

μ	=	fluid viscosity
C_p	=	fluid specific heat at constant pressure
k	=	fluid thermal conductivity
ρ	=	fluid density
β	=	coefficient of thermal expansion
g	=	gravitational constant
L	=	the natural convection length
T_w	=	wall temperature
T_b	=	bulk temperature

$$Bo = Gr / \left(\text{Re}^{3.425} \Pr^{0.8} \right)$$

For Figs 13 and 14 the wall temperature along the axis of symmetry of the front wall was used. The values of these numbers show strong buoyancy effects and their variation with tube height shows that the magnitude of these effects nearly levels off after about 3 m from the tube inlet. Because of the non-uniform heat flux, although buoyancy effects are more pronounced at the front wall, it may be more appropriate to use as a characteristic length, the tube hydraulic diameter. As the air moves up the tube and is heated up, the temperature difference between air and wall is reduced, and the use of the tube height as a characteristic length overestimates the value of the dimensionless numbers. Figures 15 and 16 show the Grashof, Rayleigh, and Buoyancy numbers computed using as a characteristic length the tube hydraulic diameter. As expected, their variation along the tube height is completely different than when the tube height was used as a characteristic length.

To assess the effect of buoyancy and property variation with temperature on the velocity distribution in an RCCS tube, simulations were performed with: (a) constant air properties (fixed at inlet values), (b) varying properties and buoyancy suppressed, (c) varying properties and buoyancy activated. These simulations where performed with the GT-MHR RCCS design with a constant reactor vessel temperature of 480 °C. Figure 17 shows the velocity distribution on the long symmetry plane of the RCCS tube at a height of 12.35 m from the inlet. This height is in the

13

zone where there is a large temperature variation along the long axis of the tube (from front to back). It is seen from this figure that the velocity variation is mainly due to the density variation with temperature, which varies significantly as we move from the front face to the back face of the tube.

In the GT-MHR design of GA, the distance between the outer surface of the reactor vessel and the front side of the RCCS tubes is 0.77 m, and the distance between the downcomer insulation and the back side of the RCCS tubes is 0.38m (GT-MHR cavity). In the NSTF facility these distances would be of the order of 0.1 m (NSTF cavity). This has an effect on the view factors between the reactor vessel and the RCCS tubes. To asses this effect on the RCSS performance parameters, simulations were performed for a reactor vessel temperature of 480 °C and a distance of 0.1 m between the reactor vessel and the front tube wall, as well as between the downcomer insulation and the back tube wall.

For the NSTF cavity, the power removed by the RCCS increased by 11%. Figures 18 and 19 show the heat transfer coefficient along the axis of the front and side RCCS walls for the "GT-MHR" and the "NSTF" cavity. These coefficients are based on the bulk air temperature. The "NSTF" cavity gives a higher heat transfer coefficient, but the difference is small. Also these Figures show sharp variations of the heat transfer coefficient near the tube inlet and outlet. Figure 20 shows the variation of the air temperature and of the tube temperature from tube-front to tube-back at a cross-section at 14.9 m from the tube inlet. The temperature variation is highly asymmetric. At this cross section the air bulk temperature is 273 °C. This temperature is higher than the air temperature next to the side wall along the back-half of this wall. It is clear that because of the highly asymmetric air temperature distribution in the tube, the use of the bulk air-temperature to compute a heat transfer coefficient is not meaningful. Instead, the heat transfer coefficient based on the air temperature in the cells next to the wall is more meaningful. This heat transfer coefficient for the front, side and back wall of the tube is shown in Figs. 21, 22 and 23. The difference, in terms of the heat transfer coefficient, between the "GT-MHR" cavity and the "NSTF" cavity is very small.

The buoyancy driven flow in the reactor cavity does not converge to a steady state (laminar as well as turbulent simulation with the steady state simulator), because the flow may be chaotic. The following figures show air velocity distributions in the "NSTF" cavity assuming laminar flow in the cavity. The simulation with the high Re number k-ε model gives similar results. As Figure 24 shows (a vertical cross section of the cavity through a tube), the flow moves down in the space between the downcomer insulation and the tubes and upwards in the space between the reactor vessel and the tubes. Figure 25 shows velocity contours for the whole cavity assuming laminar flow, and Figure 26 shows the same information as predicted by the high-Re number k-ε model. The maximum velocity is about 1m/sec. Figure 27 shows the velocity distribution in a vertical cross section of the cavity in the gap between two tubes. It clearly shows a complicated flow pattern that may be generated by a chaotic flow. To ascertain that the flow is chaotic a transient simulation is needed.

3.2 RCCS Performance at VHTR Conditions

 Uniform Reactor Vessel Temperature of 560° C

For a reactor vessel temperature of 560 °C, the buoyancy force driving the RCCS flow established an air flow rate of 5.223 e-02 kg/sec per RCCS tube. This corresponds to a Re number of 20,030, versus a Re number of 18,780 for the RCCS of the GT-MHR design. The RCCS (292 tubes) removed 5.02 MW versus 3.3 MW removed by the RCCS of the GT-MHR.

Figure 28 shows the temperature distribution on a tube cross-section at 14.9 m from the tube inlet (tube outlet at 15.6m). It is similar to the corresponding distribution for a reactor vessel temperature of 480 °C (Fig. 8). It is very asymmetric, it reaches a minimum around the center of the back half of the tube, and the maximum to minimum difference is 104 °C. versus 137 °C for a reactor vessel temperature of 480 °C. The temperature distribution on the front and back walls of the tube are nearly uniform, but there is a large temperature variation from front to back on the side wall of the tube. This variation is about 111 °C.

Figure 29 shows the heat transfer coefficient along the axis of the front, side and back tube walls as predicted by the high-Re number model of turbulence. These heat transfer coefficients are based on the fluid temperature next to the wall. The variation of the heat transfer coefficient along the tube height is similar to that for a 480 °C reactor vessel temperature, and for the higher reactor vessel temperature the heat transfer coefficient is up to 20% higher.

Figure 30 shows the variation of the heat transfer coefficient around the tube wall at 14.9 m from the tube inlet. This variation is also similar to that for a reactor vessel temperature of 480 °C.

Peak Reactor Vessel Temperature of 560 °C

The analyses presented up to this point were based on the assumption of a uniform reactor vessel temperature. To assess the effect of a non-uniform reactor vessel temperature on the RCSS performance parameters, simulations were also performed with a non-uniform reactor vessel temperature as shown in Table 1. This section presents the results of an analysis for the reactor vessel temperature distribution shown in Table 1 having a peak value of 560 °C. This distribution is similar to a distribution provided in Ref. 7.

Figure 31 shows the heat transfer coefficient along the RCCS tube height. Its value starts to level off after about 7 m, and its variation is within the range predicted for a uniform reactor vessel temperature, and the range covered by NSTF (section 4.0). Figure 32 shows the Nusselt number along the axis of the front, side, and back tube walls. Its value starts to level off after about 7 m, and its variation is nearly within the range predicted for a uniform reactor vessel temperature, and the range covered by NSTF (section 4.0). Figures 33 and 34 show the Grashof, Rayleigh and Buoyancy numbers along the axis of the front side of the tube. Their variation is well within the range covered by NSTF (section 4.0). These numbers are based on treating the front wall of the RCCS tubes as a vertical plate and using as characteristic length the height of the plate (this treatment was applied only in the use of the characteristic length).

Figures 35 and 36 show the Grashof, Rayleigh, and Buoyancy numbers computed using as a characteristic length, the tube hydraulic diameter. As expected, their variation along the tube height is completely different than when the tube height was used as a characteristic length. The Grashof and Rayleigh numbers vary between about 10e05 and 10e8.5, and the Buoyancy number between 10e-09 and 10e-6. The higher values of these numbers are more important, and NSTF (section 4.0) covers well these values.

VHTR Design with a Variable Reactor Vessel Temperature

A VHTR design with a core outlet temperature of 1000 °C, developed at INEEL, was analyzed with RELAP at ANL (HPCC and LPCC transients). The LPCC transient gives a higher peak fuel temperature, which is reached at 76.7 hr from transient initiation. RELAP predicted an RCCS flow rate of 13.32 kg/s at 76.7 hrs. The RCCS performance of this design, called here reference

VHTR design, was analyzed with STAR-CD at 76.7 hrs using the flow rate and the outer reactor vessel temperature distribution predicted by RELAP (Fig. 37). This distribution has a peak value of 467 °C at 6 m from the bottom of the lower reflector (floor of reactor cavity), and drops significantly below and above this location.

The temperature distribution of the front (hottest) tube wall reaches a peak value of 552.5 K (279.5 °C) at 6.8 m. Figure 38 shows the air temperature distribution along the RCCS tube, and Figure 39 shows the air and tube temperature distribution on a tube cross section at a height of 5.3 m (around the area of the peak wall temperature). The wall temperature around the tube varies by about 111 °C, while the air temperature varies by about 122 °C. Figure 40 shows the variation of the heat transfer coefficient along the axis of the front, side, and back tube walls. This variation is covered well by the variation of the same variables at NSTF (section 4.0). Figures 41, 42, and 43, show the variation of the Nusselt number, Grashof and Rayleigh number, and of the buoyancy number. Their variation is also well covered by the variation of the same parameters at NSTF (section 4.0). Notable is the sharp drop of the Grashof, Rayleigh, and buoyancy numbers after a height of about 8 m (reactor vessel temperature peaks at 6 m).

4.0   NSTF PERFORMANCE

In the effort to demonstrate that all significant fluid flow and heat transfer phenomena in the RCCS, and the range of variation of the parameters describing these phenomena can be simulated at NSTF, NSTF simulations were performed for: (a) a uniform heated wall temperature of 480 °C, and (b) for a uniform heated wall temperature of 677 °C

4.1   Uniform Heated Wall Temperature of 480 °C

For this simulation, the air velocity at the tube inlet was set to 4.353 m/s, based on a GT-MHR RCCS flow rate of 14.3 kg/s at steady state conditions. For a uniform heated wall temperature of 480 °C, it was computed (from the pressure drop model of section 2.3) that the pressure losses at NSTF can accommodate a larger flow rate than that corresponding to an air velocity of 4.353 m/s. Thus, the velocity of 4.353 m/s can be achieved at NSTF by properly adjusting the pressure drop damper. At the outer surface of the insulation a constant temperature of 43 °C was used as a boundary condition. The air inlet temperature was also set to 43 °C (GA RCCS air inlet temperature).

This simulation predicted an air outlet temperature (bulk) of 181.5 °C, a reactor vessel heat flux of 10.14 kw/m2, and a heat removal rate of 6.9 kw/tube. Figure 44 shows the air and tube-wall temperature distribution at the top of the heated section (6.7m). The tube temperature varies from 620 K (front) to 514 K (back), while the air temperature varies from 411 K to 579 K. These temperatures variations are similar to those near the outlet of the RCCS tubes for the same reactor vessel temperature. Figure 45 shows the variation of the heat transfer coefficient along the axis of the front, side and back tube walls. This variation is also similar to that in the RCCS. Figures 46 and 47 show the variation of the heat transfer coefficient and of the heat flux around the tube. Figure 48, shows the variation of the heat transfer coefficient assuming a constant air thermal conductivity. Figures 45 and 48 show that the increase in the heat transfer coefficient with tube height is due to the increase in the thermal conductivity of air as its temperature increases.

Figure 49 shows the variation of the Reynolds (Re) number along the tube height. For a reactor vessel temperature of 480 °C, the variation of the Re number in the plant RCCS tube and the NSTF tube is nearly identical. However, because the plant RCCS tube is longer, in plant RCCS

the Re number drops further down to about 12000 at the top of the tube. As Figure 49 shows, and as it will be discussed later, such lower values can also be simulated at the NSTF for an inlet air velocity of 4.52 m/s, and a heated wall temperature of 950 K (677 °C).

Figures 50 and 51 show the variation of the Grashof, Rayleigh and Boyancy numbers along the height of the front wall of the NSTF tube for a heated wall temperature of 480 °C. In these plots, the front wall has been treated as a vertical heated plate and the height of the plate is used as a characteristic length. The variation of these numbers is very similar as that in the RCCS tube with the only difference that the upper value of these numbers is slightly higher in the RCCS tube (longer tube).

Figure 52 shows the Nusselt number along the tube wall at NSTF. Its variation is very similar to that in the RCCS tube for a uniform reactor vessel temperature of 480 °C (Fig. 12), with a slightly lower limit value in the RCCS tube (longer tube).

Figures 53 and 54 show the Grashof, Rayleigh and Buoyancy numbers computed using the hydraulic diameter as a characteristic length.

4.2. Uniform Heated Wall Temperature of 677 °C

The NSTF facility was originally intended to be used for RVACS simulations with a reactor vessel temperature up to 950 K (677 °C), although the heater plates can provide much higher temperatures. An NSTF simulation was performed with a uniform heated wall temperature of 677 °C. To determine the tube flow rate under natural convection, pressure boundary conditions were used at the inlet and outlet of the tube. Since the flow is nearly incompressible, only the pressure difference is of importance. After the inlet pressure was fixed, the pressure at the outlet of the tube was determined by considering the buoyancy force in the NSTF stack (15.2 m), and the pressure losses at the inlet and outlet of the tubes, along the stack and at the stack outlet.

The simulation predicted an inlet air velocity of 5.055 m/s, a bulk air temperature at the tube outlet of 297.8 °C, a heat removal rate per tube of 14.755 kw, and a heated wall heat flux of 21.7 kw/m2. Figure 55 shows tube and air temperature distributions at the tube outlet (6.7 m). The tube temperature varies from 822 K (front) to 666 K (back of tube side), while the air temperature varies from 505 K to 737 K. These temperature variations are significantly higher than those predicted for a heated wall temperature of 480 °C. Figure 56 shows the variation of the heat transfer coefficient along the axis of the tube walls. The maximum values of these coefficients are above those of the plant RCCS for a reactor vessel temperature of 480 °C, and very close to those for a reactor vessel temperature of 560 °C. Thus, NSTF operation to 677 °C covers the whole range of heat transfer coefficient variation in the plant RCCS.

Figure 49 shows that NSTF operation at 677 °C covers the upper range of the plant RCCS Re number. Figures 57, and 58 show the variation of the Grashof, Rayleigh, and Buoyancy numbers along the height (axis) of the front tube wall (the tube height was used as a characteristic length). They vary very similarly as in the case of a heated wall temperature of 480 °C. Figures 59 and 60 show the same parameters (Grashof, Rayleigh, and Buoyancy numbers) computed using the hydraulic diameter as a characteristic length.

 Figure 61 shows the Nusselt number along the axis of the NSTF tube walls, while Figure 62 shows the same information along the RCCS tube wall for a uniform reactor vessel temperature of 560 °C. These Figures and Figures 12 and 52 show that NSTF covers well the range of Nusselt number variation in the RCCS.

As Figure 49 shows, in the plant RCCS as the air is heated up in the tubes its viscosity increases and the Re number drops at the top of the tube at a value of 12000. Such low Re number values can also be simulated in the NSTF (shorter tube) by increasing the flow pressure losses and reducing the flow rate. For example, as Figure 49 shows, for a heated wall temperature of 677 °C and an air inlet flow rate of 4.52 m/s the Re number along the NSTF tube varies from 17300 to 11900 which covers well the range of Re number variation in the RCCS.

5.0   CONCLUSIONS

In the RCCS, strong 3-D effects result in large heat flux, temperature, and heat transfer variations around the tube wall. Higher temperatures in the front tube wall and air density variations with temperature lead to significant buoyancy inside the tube which reduces turbulence, thermal mixing, and the overall heat transfer coefficient. The increase in air thermal conductivity with temperature results in an increase of the heat transfer coefficient with tube height. The increase of viscosity with temperature leads to a significant decrease of the Reynolds number with tube height. Radiation between the RCCS tube walls redistributes the heat flux. There is a large difference in the heat transfer coefficient predicted by turbulence models and heat transfer correlations, and this underscores the need of experimental work to validate the thermal performance of the RCCS.   Simulations of the RCCS at the NSTF facility can cover all important fluid flow and heat transfer phenomena, and the whole range of variation of the important thermal-hydraulic parameters in the RCCS.

Reference:

1.0 Gas Turbine-Modular Helium Reactor (GT-MHR) Conceptual Design Description Report, Revision 1, GA Project No 7658,General Atomics, San Diego,CA (1996). (nov)

2.0 C. P. Tzanos, "Passive Decay Heat Removal in the Reactor Cavity Cooling System," Trans. Am. Nucl. Soc., November 2004.

3.0 B. S. Petukhov and A. F. Polyakov, Heat transfer in Turbulent Mixed Convection, Hemisphere Publishing Company,1988 (nov)

4.0 P. D. Bayless, "VHTR Thermal-Hydraulic Scoping Analyses Using RELAP5-3D/ATHENA", Global 200, pp 312-319, New Orleans, LA, November 16-20,2003.

5.0 NGNP Point Design - Results of the Initial Neutronics and Thermal-Hydraulic Assessments During FY-03. INEEL/EXT-03-00870 Rev.1. (oct wei)

6.0 J. D. Jackson, M. A. Cotton and B. P. Axcell, "Studies of Mixed Convection in Vertical Tubes," Int. J. Heat and Fluid Flow, 10, pp 2-15 (1989)

7.0 Heat Transport and Afterheat Removal for Gas Cooled Reactors Under Accident Conditions, IAEA-TECDOC-1163, IAEA-Vienna, 2000 (jan)

Table 1. Reactor vessel temperature distribution (° C) – Peak vessel temperature of 560 °C

Height, m	Temperature Distribution
0 – 4.0	linear from 400 to 560
4.0 – 6.73	560 uniform
6.73 – 10.73	linear from 560 to 380
10.73 – 15.60	linear from 380 to 280
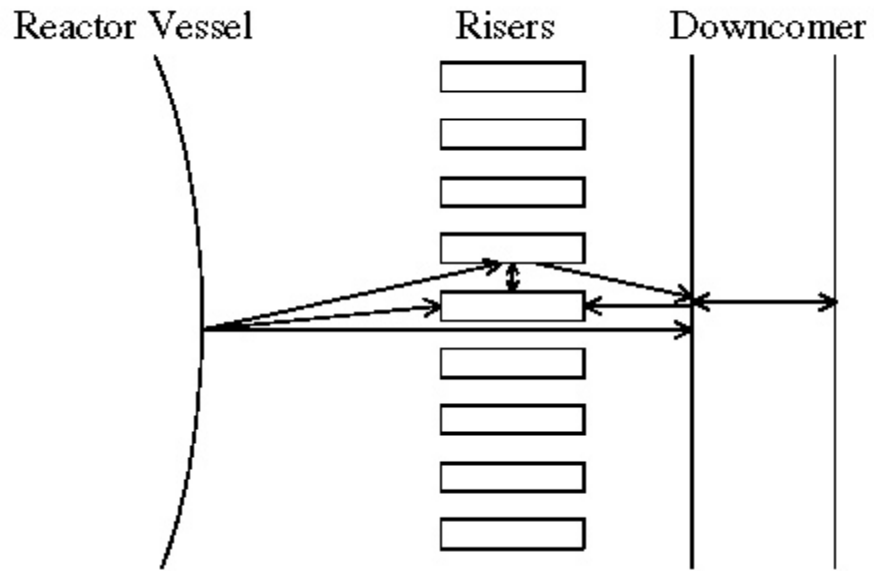
Figure 1. Horizontal cross-section of the GT-MHR RCCS
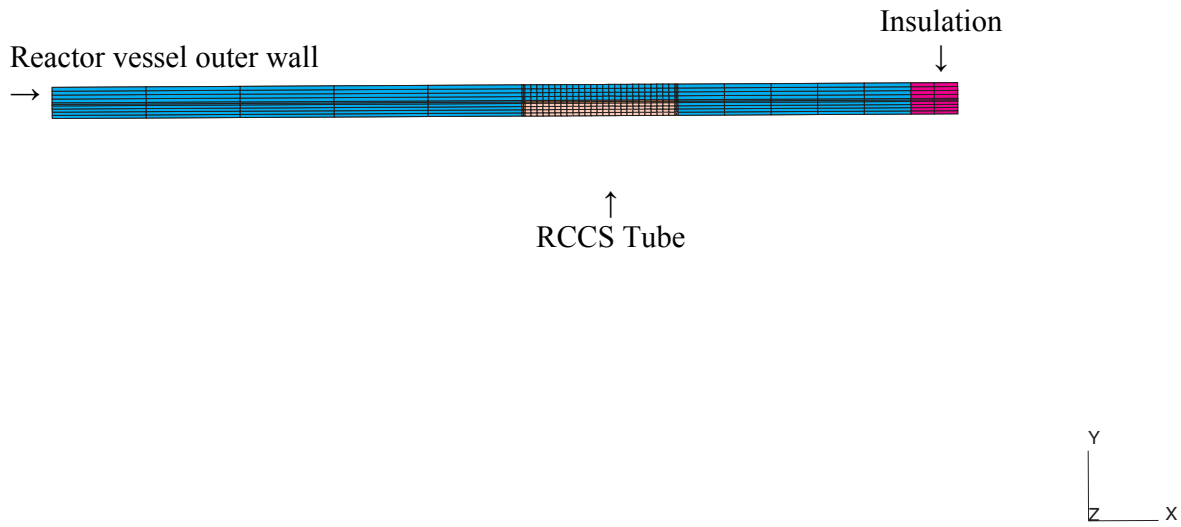
Figure 2. Cross-section of simulated RCCS configuration (plant geometry)
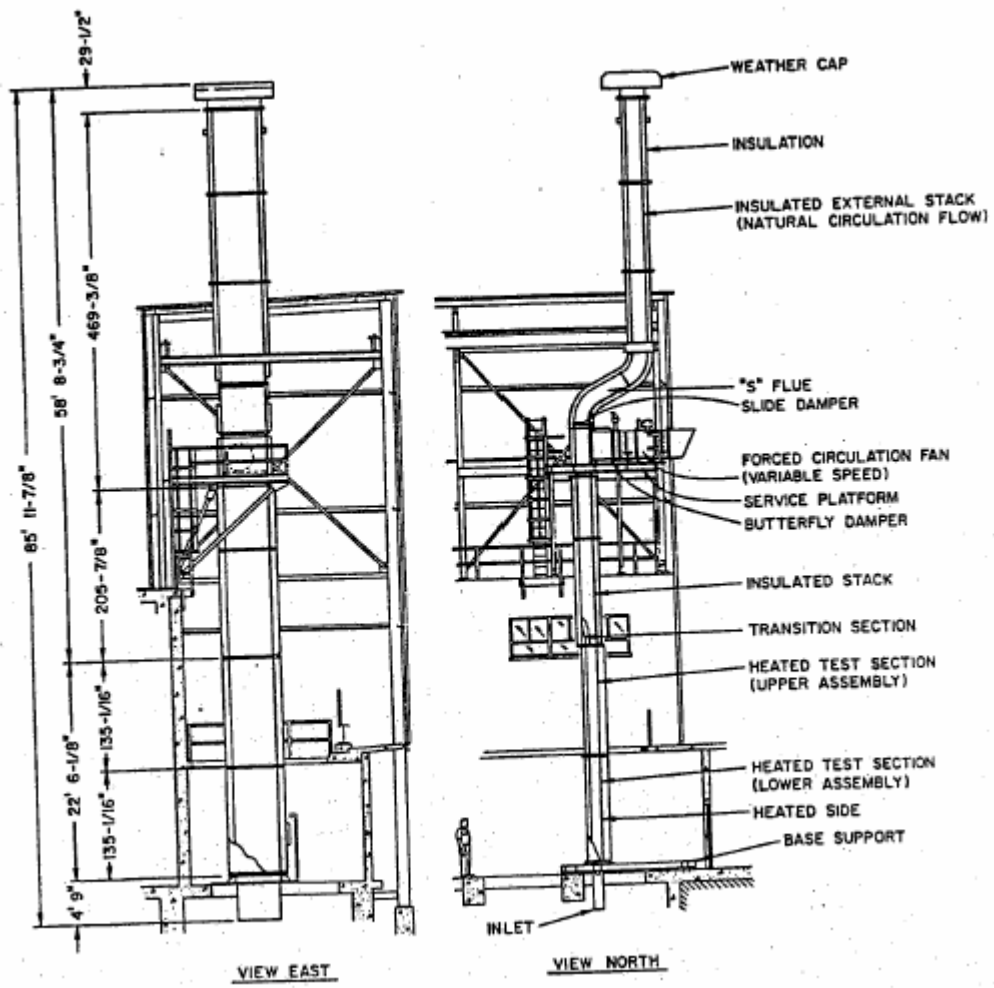
Figure 3. NSTF test assembly
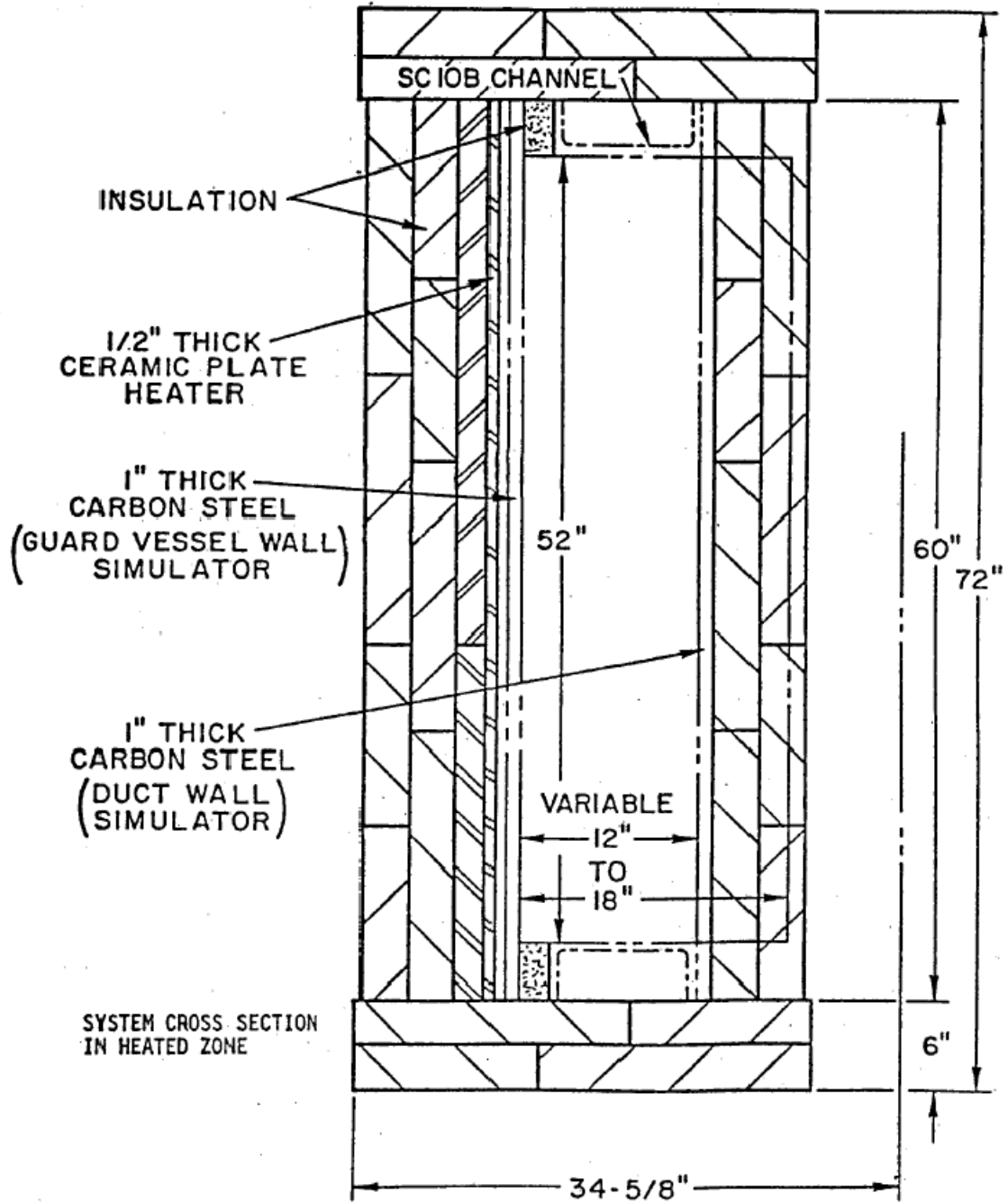
Figure 4. NSTF test section
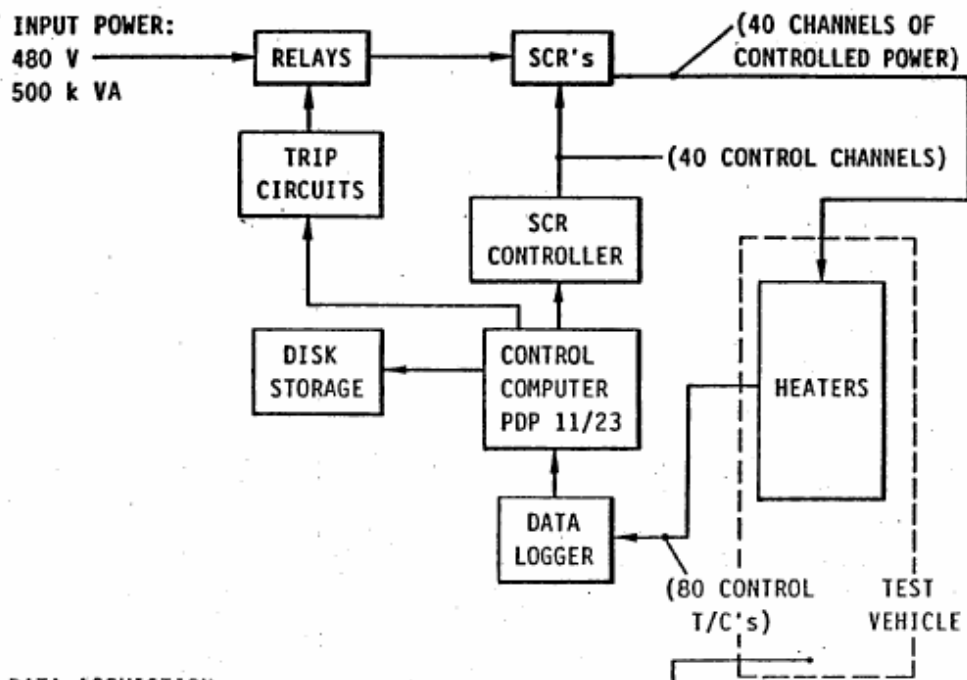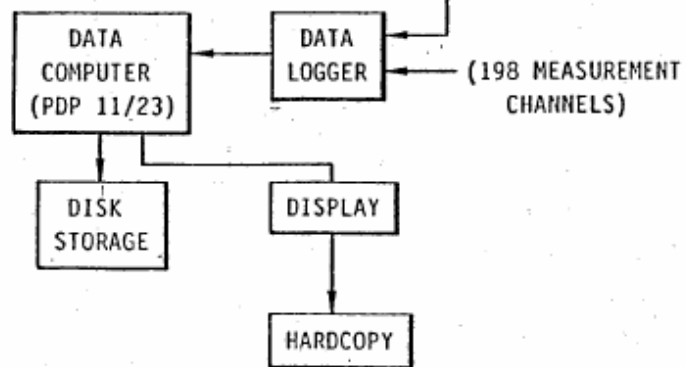
Figure 5. Heater Control and Data Acquisition System block diagram
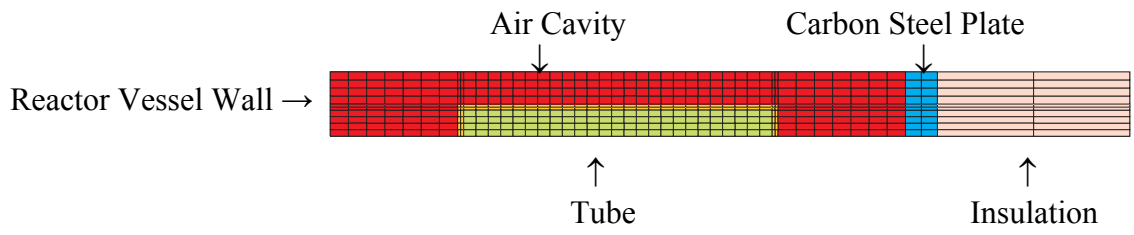
Figure 6. Cross-section of RCCS model at NSTF
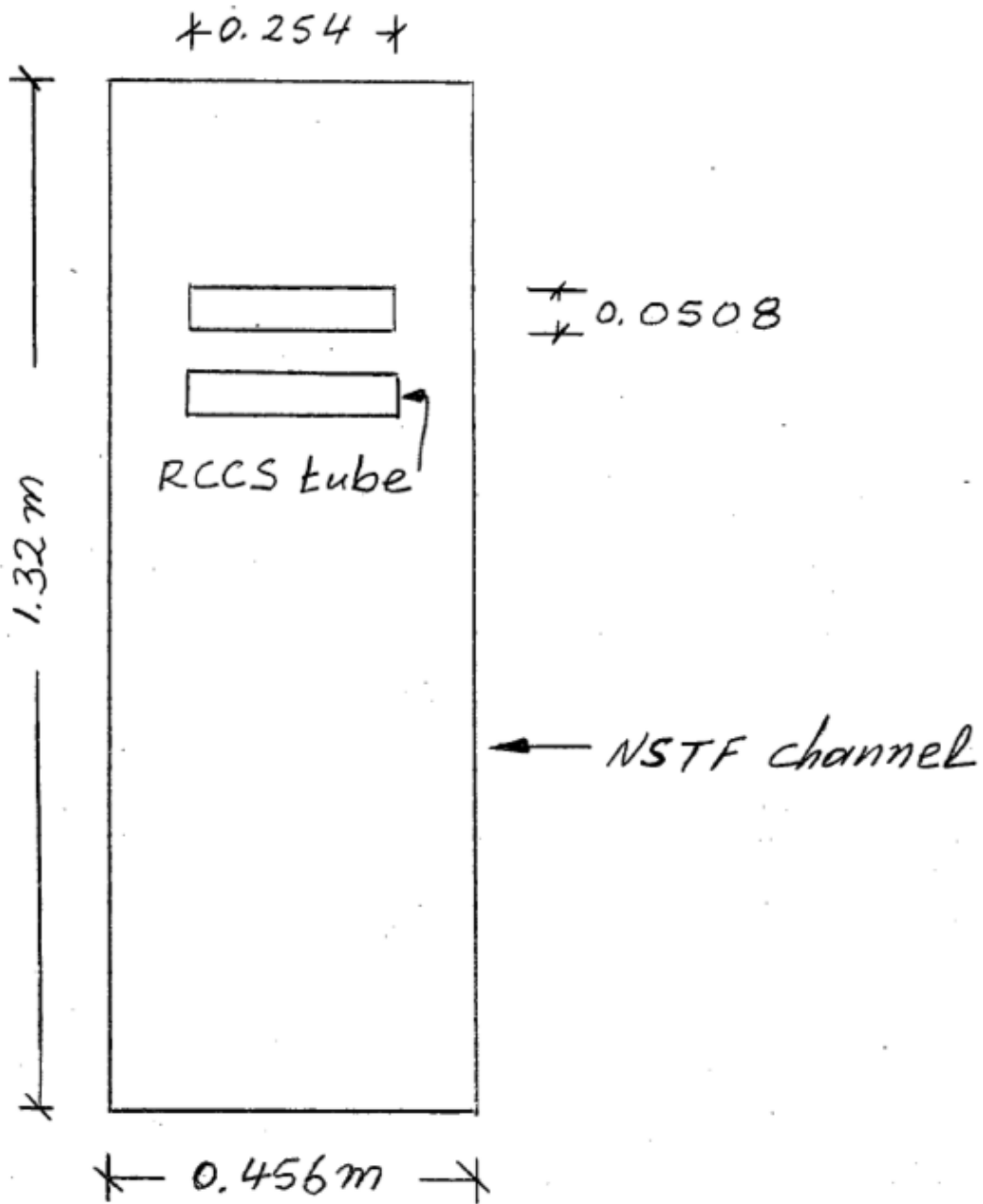
Figure 7. NSTF channel with RCCS tube
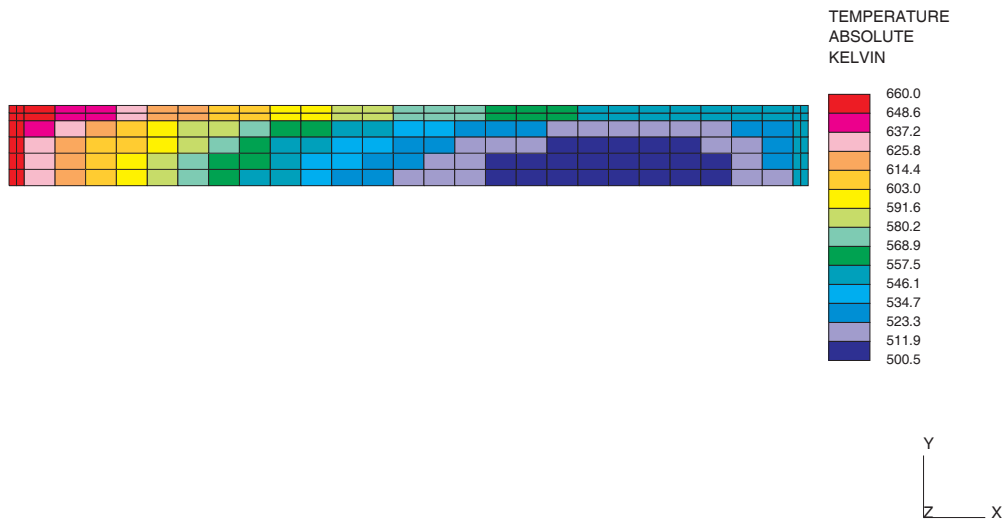
Figure 8. Tube temperature distribution at 14.9 m, reactor vessel temperature of 480 °C
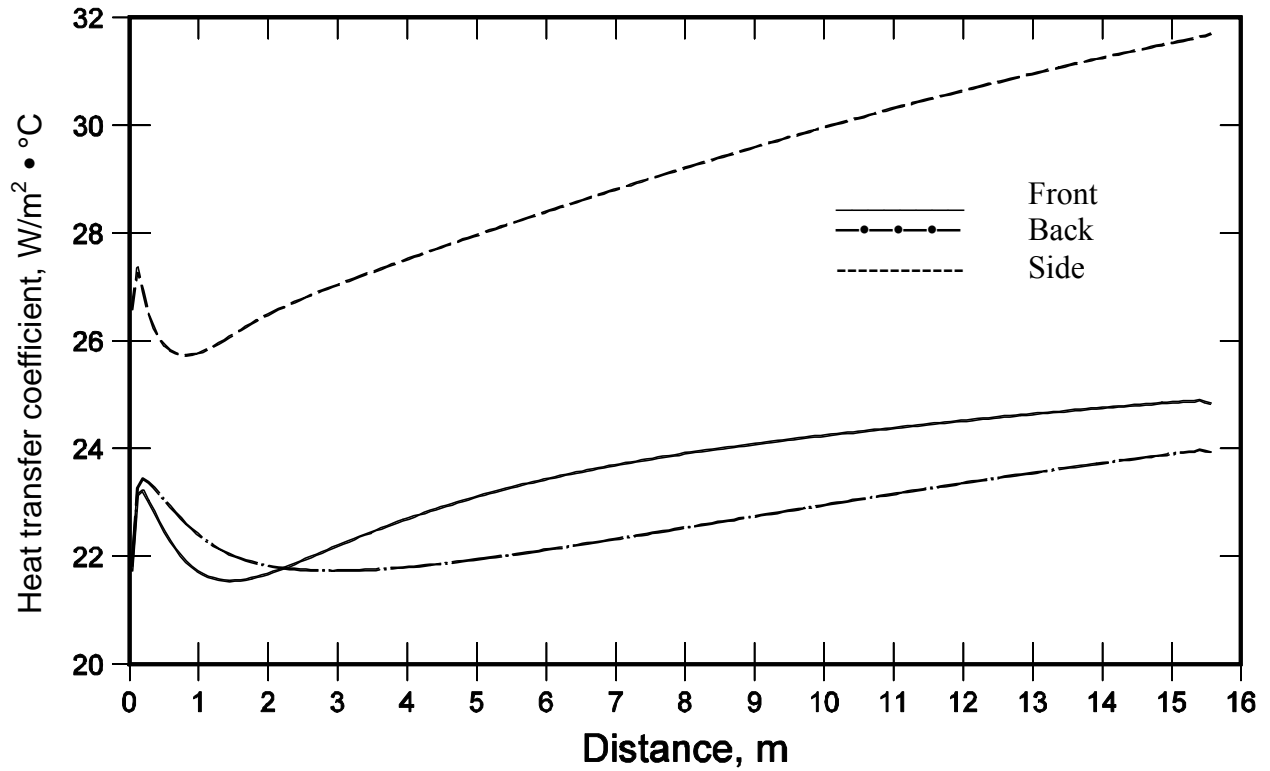
Figure 9. Heat transfer coefficient for reactor vessel temperature 480°C.
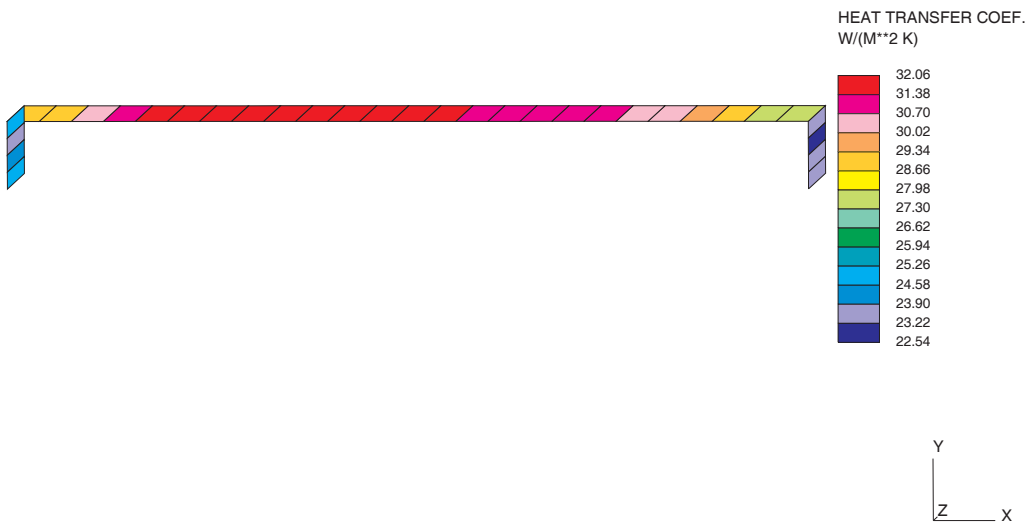
Figure 10. Heat transfer coefficient variation around the tube at 14.9 m, reactor vessel temperature of 480 °C

a: heat flux at 1.0 m

b: heat flux at 7.8 m

c: heat flux at 14.9 m
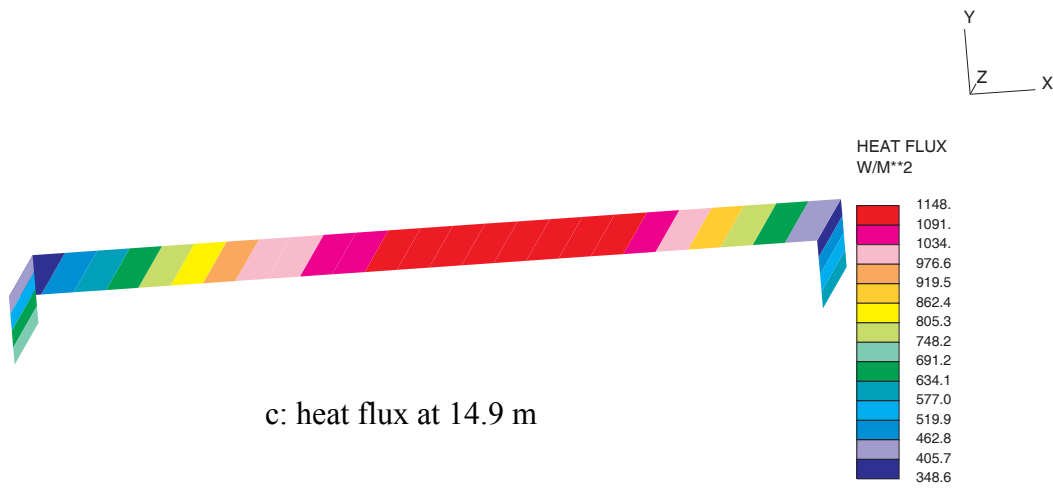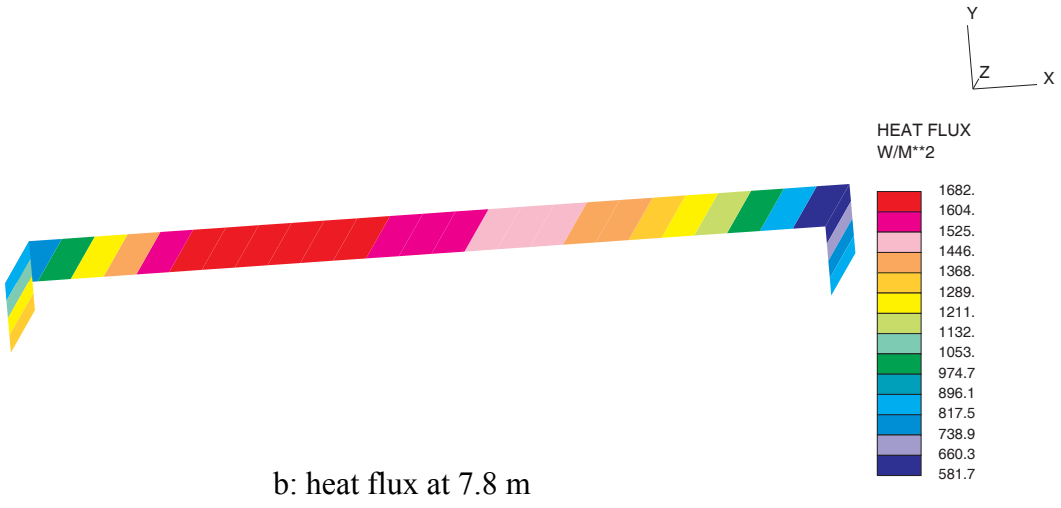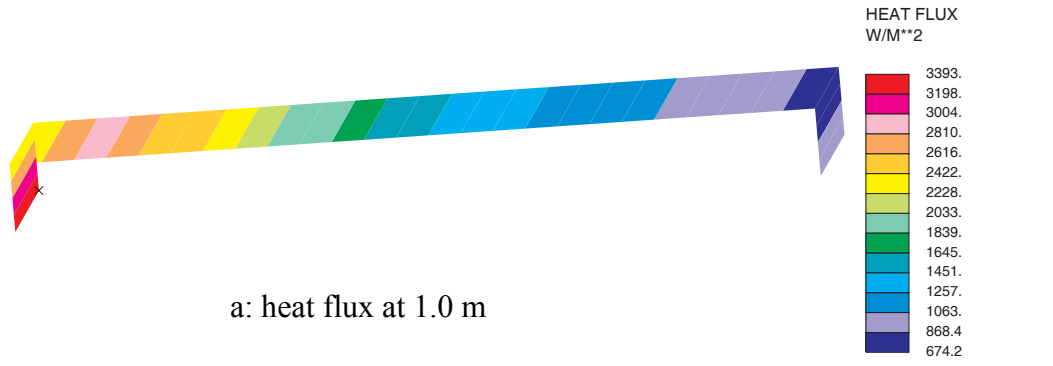
Figure 11. Heat flux distribution, reactor vessel temperature of 480 °C.

28
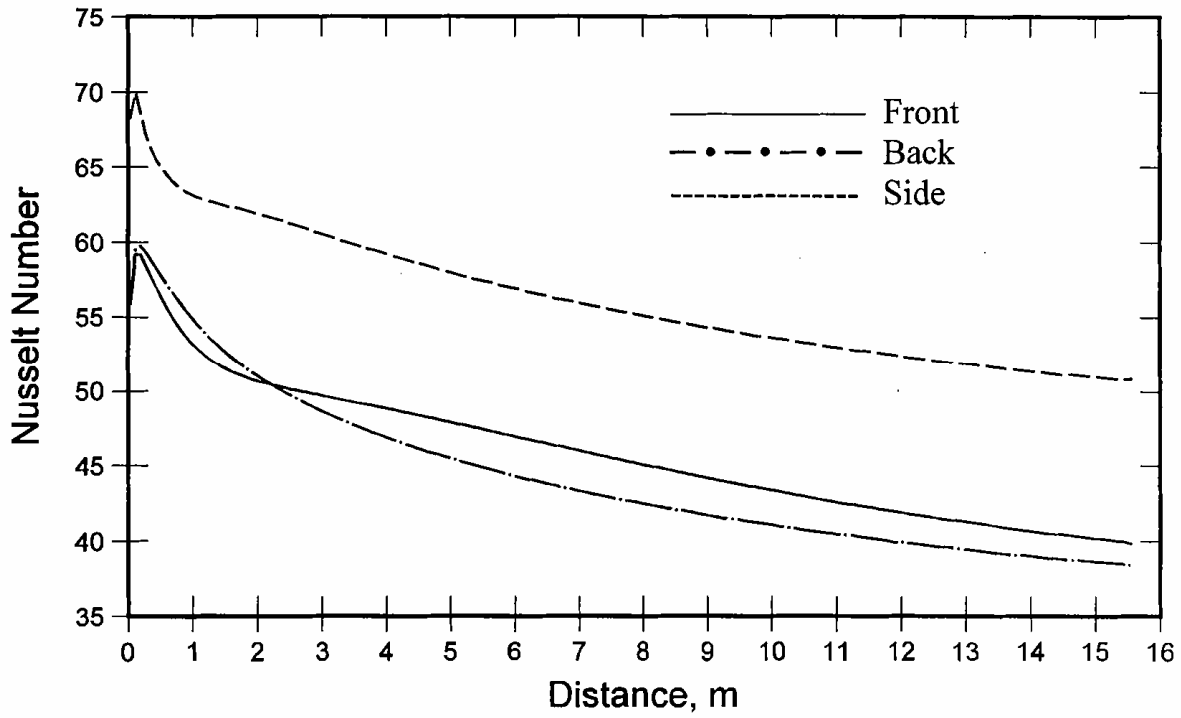
Figure 12. Nusselt number versus RCCS tube height, reactor vessel temperature of 480 °C
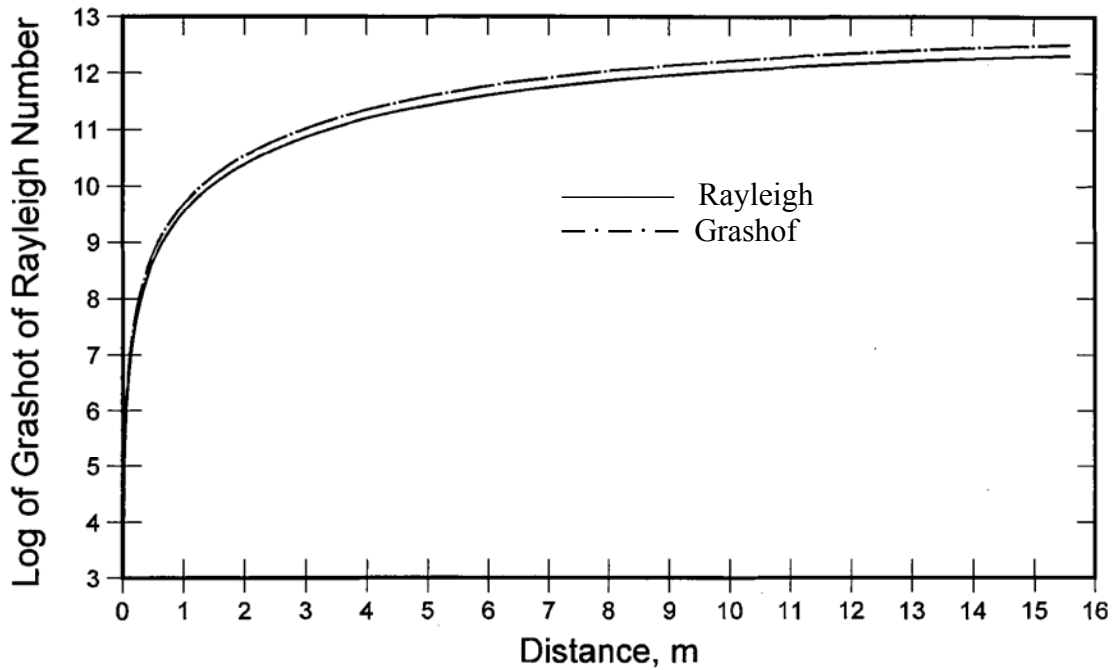
Figure 13. Rayleigh and Grashof Number, reactor vessel temperature of 480 °C
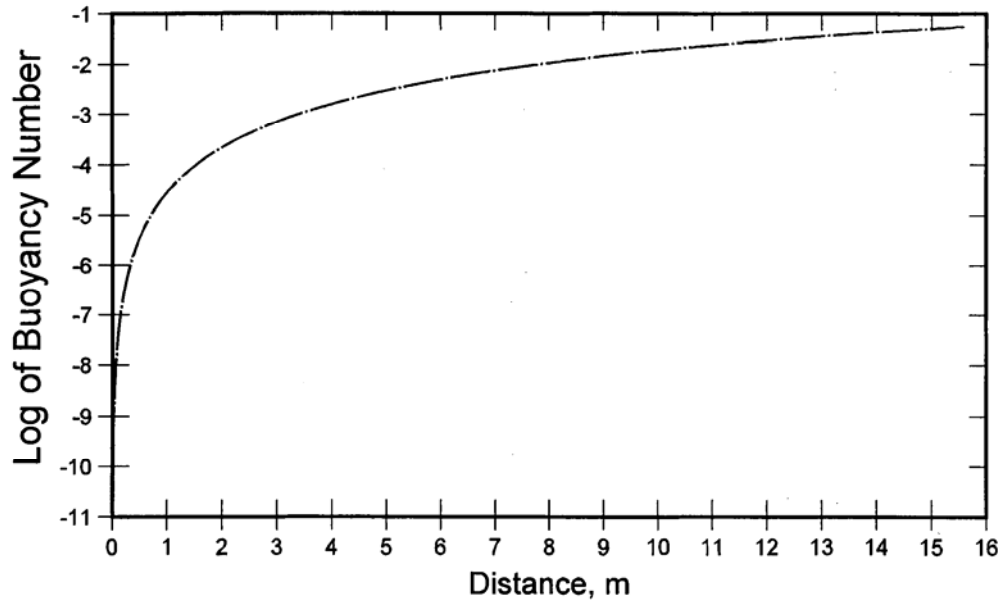
Figure 14. Buoyancy Number, reactor vessel temperature of 480 °C
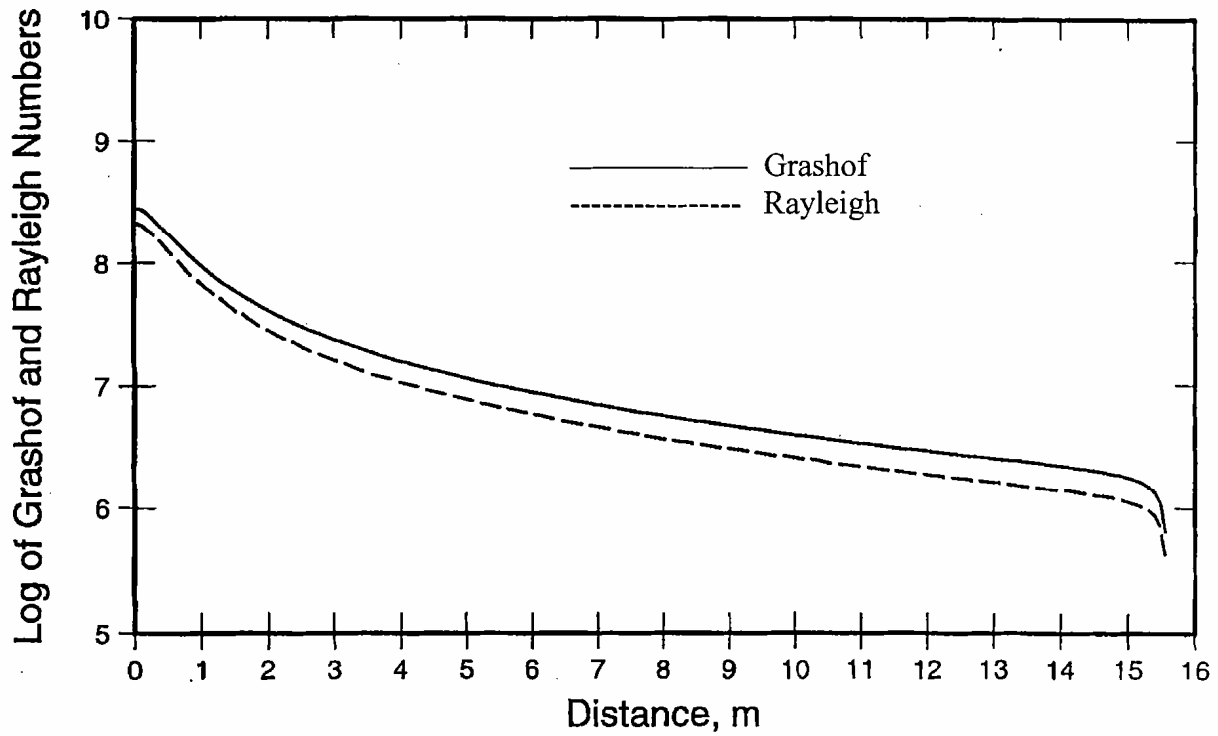
Figure 15. Grashof and Rayleigh numbers along the axis of the front RCCS tube wall (based on hydraulic diameter, and reactor vessel temperature of 480 °C).
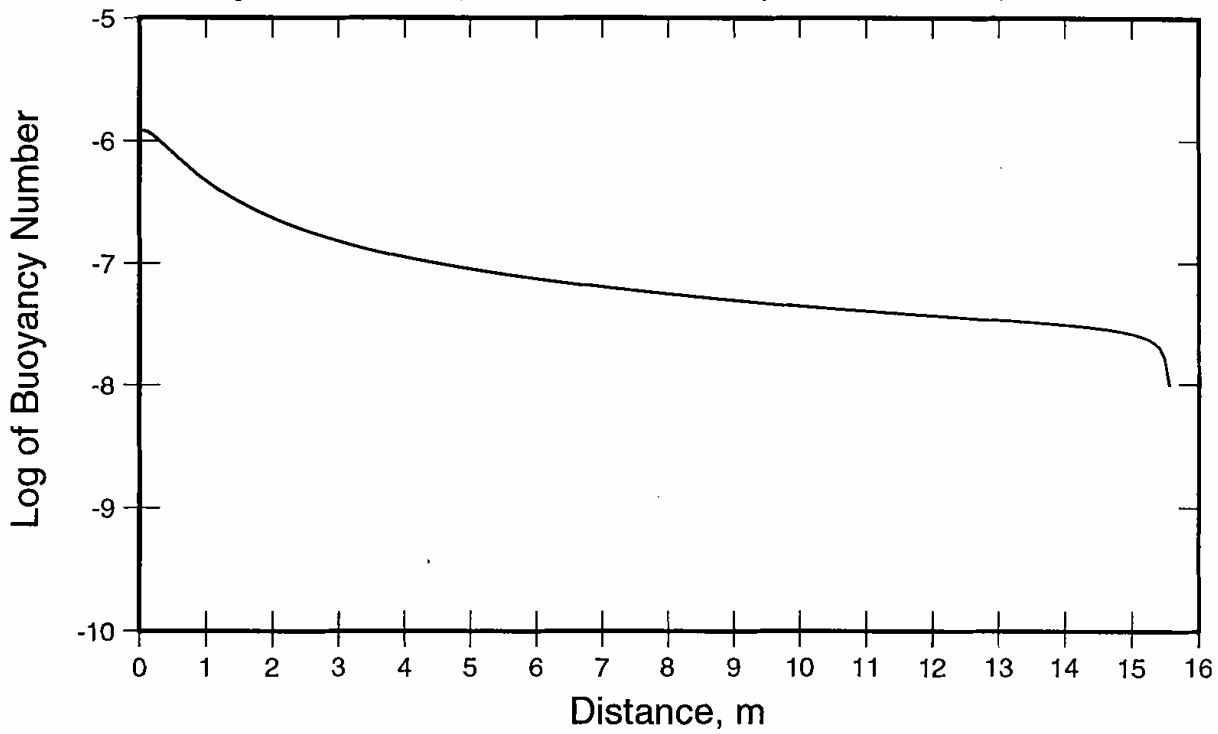
Figure 16. Buoyancy number along the axis of the front RCCS tube wall (based on hydraulic diameter, and reactor vessel temperature of 480 °C).
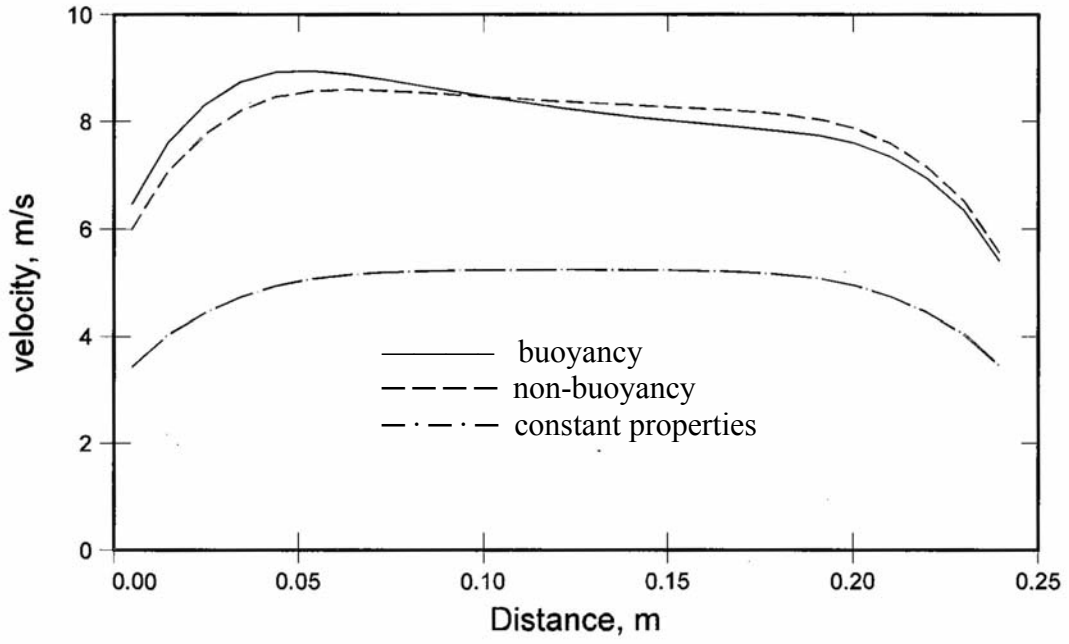
Figure 17. Velocity distribution at 12.35 m for reactor vessel temperature of 480 °C
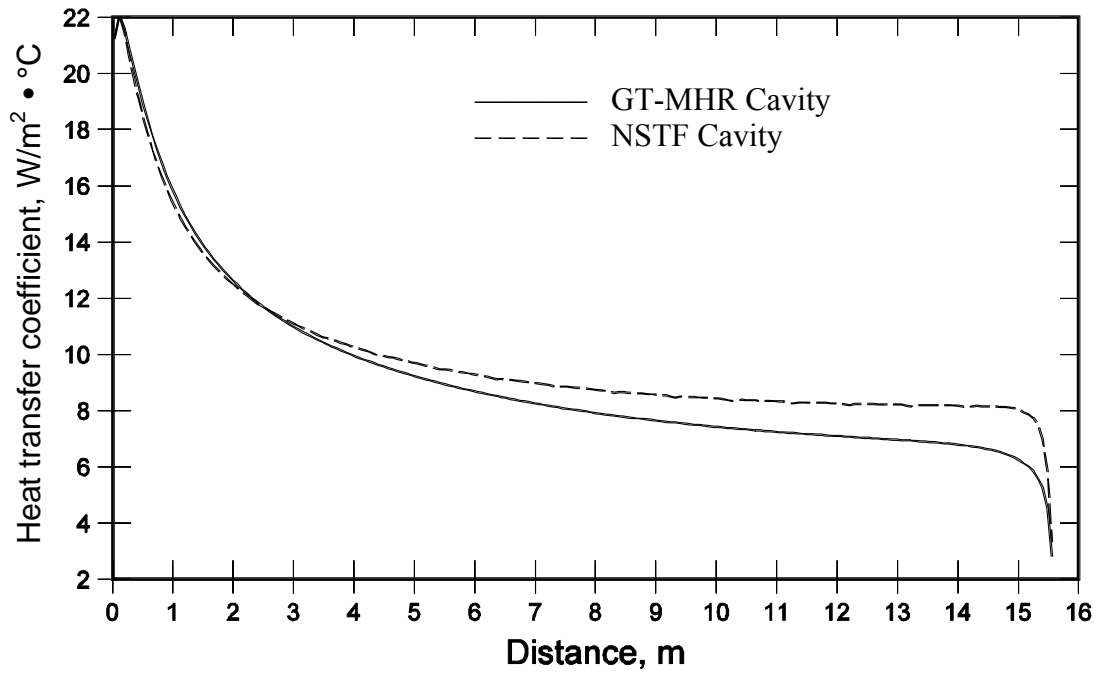
Figure 18. Cavity parametrics: heat transfer coefficient on the front wall (based on bulk temperature)
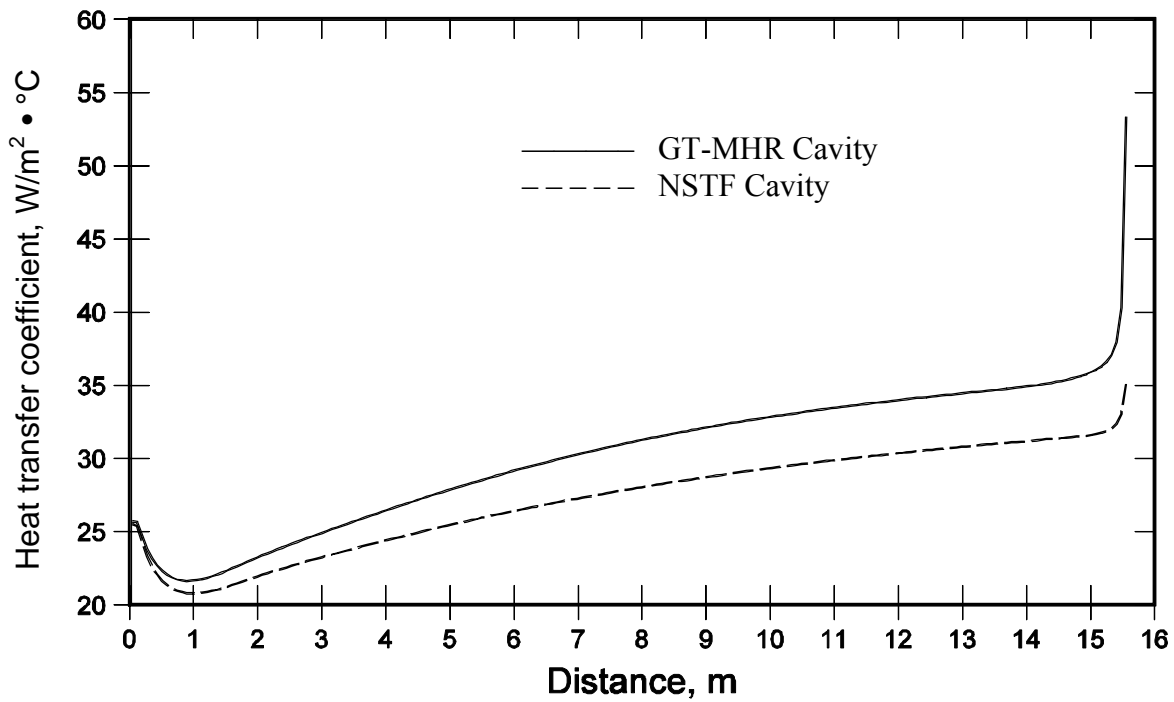
Figure 19. Cavity Parametrics: heat transfer coefficient on the side wall (based on bulk temperature)
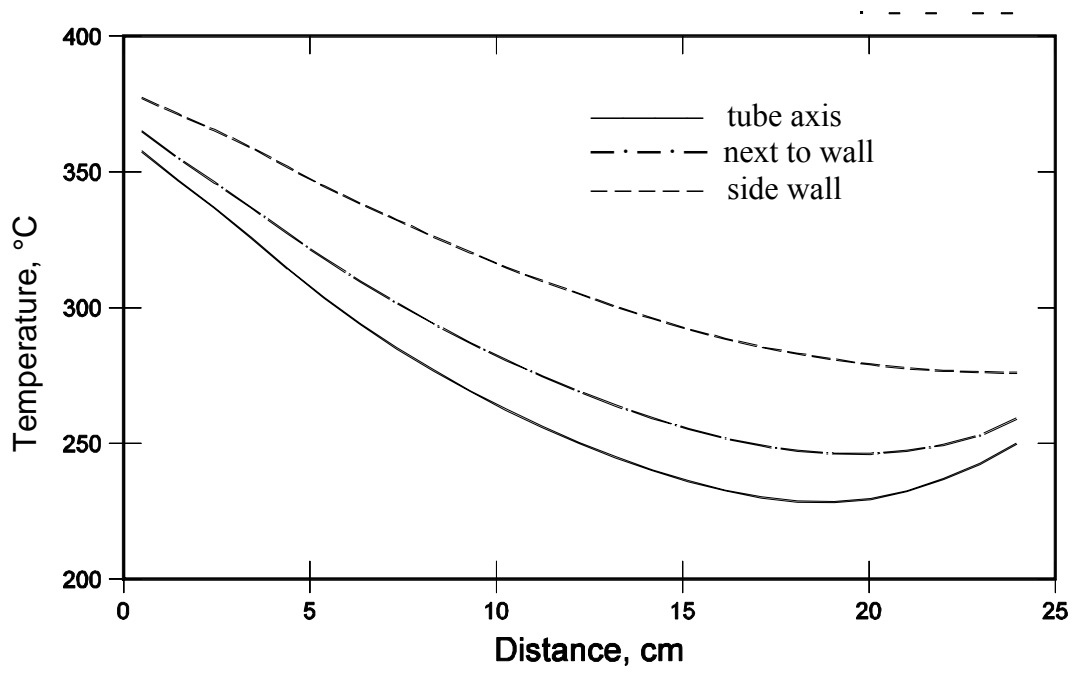
Figure 20. Air and tube wall temperature variation at 14.9 m (GT-MHR cavity)
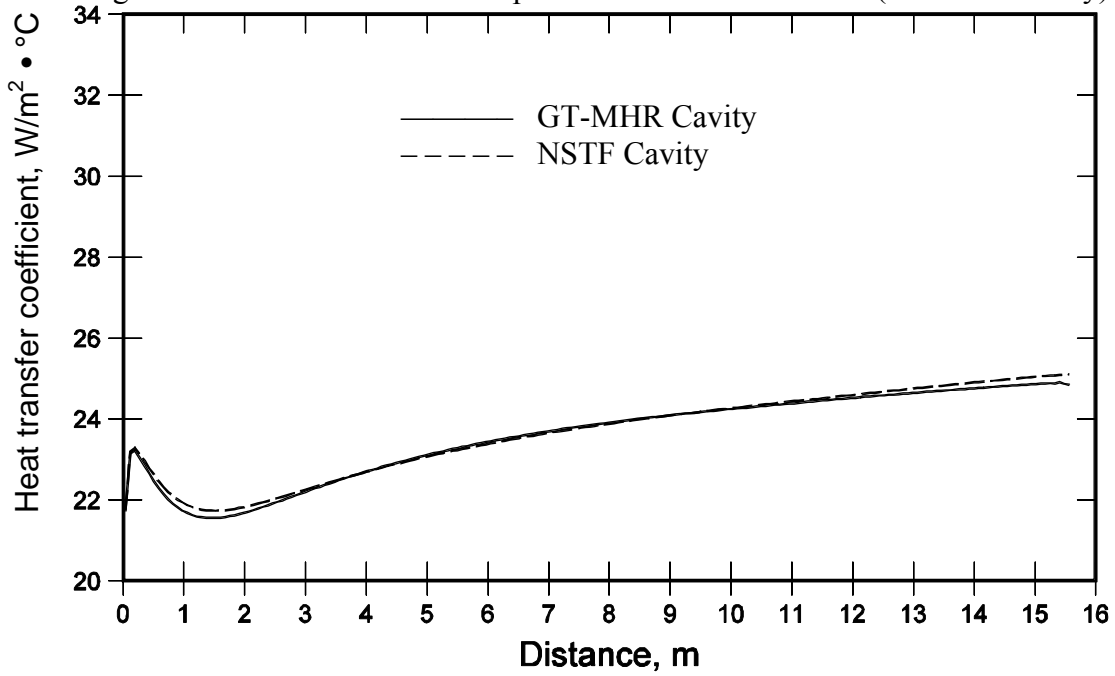
Figure 21.Cavity parametrics: heat transfer coefficient along the axis of the front wall

34
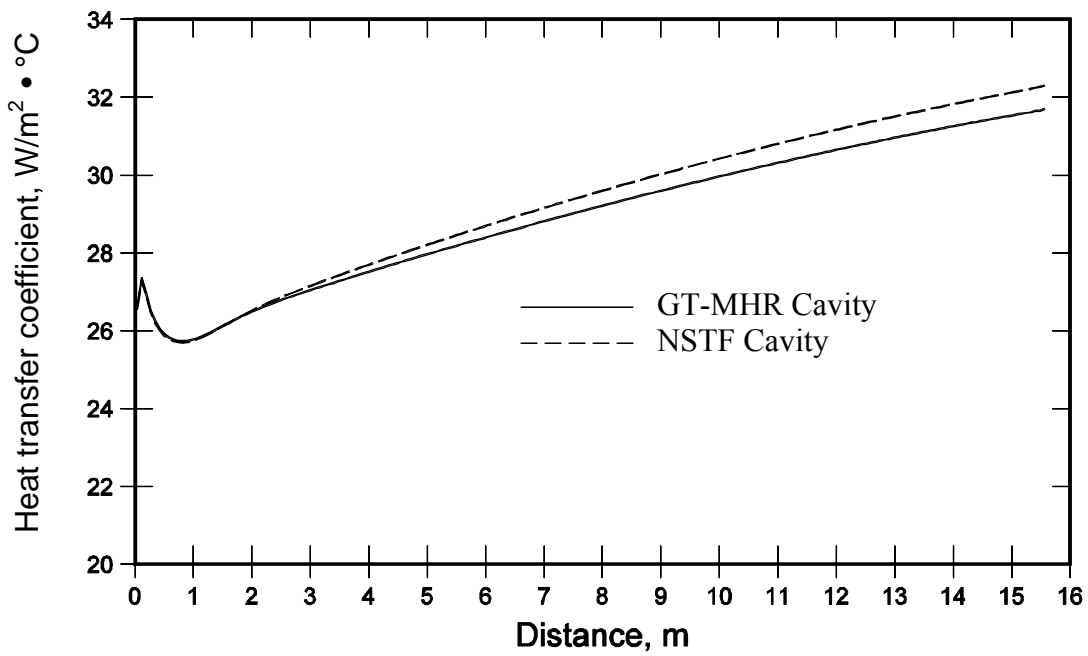
Figure 22. Cavity parametrics: heat transfer coefficient along the axis of the side wall
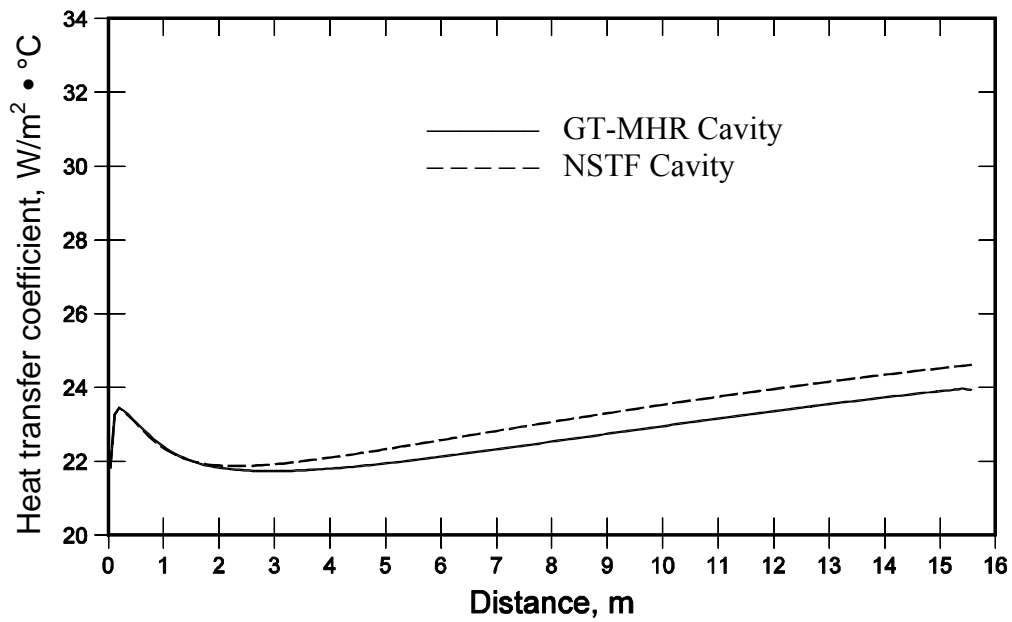
Figure 23. Cavity parametrics: heat transfer coefficient along the axis of the back wall

VELOCITY MAGNITUDE
M/S

	1.085
	1.007
	0.9302
	0.8530
	0.7758
	0.6986
	0.6214
	0.5442
	0.4670
	0.3899
	0.3127
	0.2355
	0.1583
	0.8109E-01
	0.3903E-02
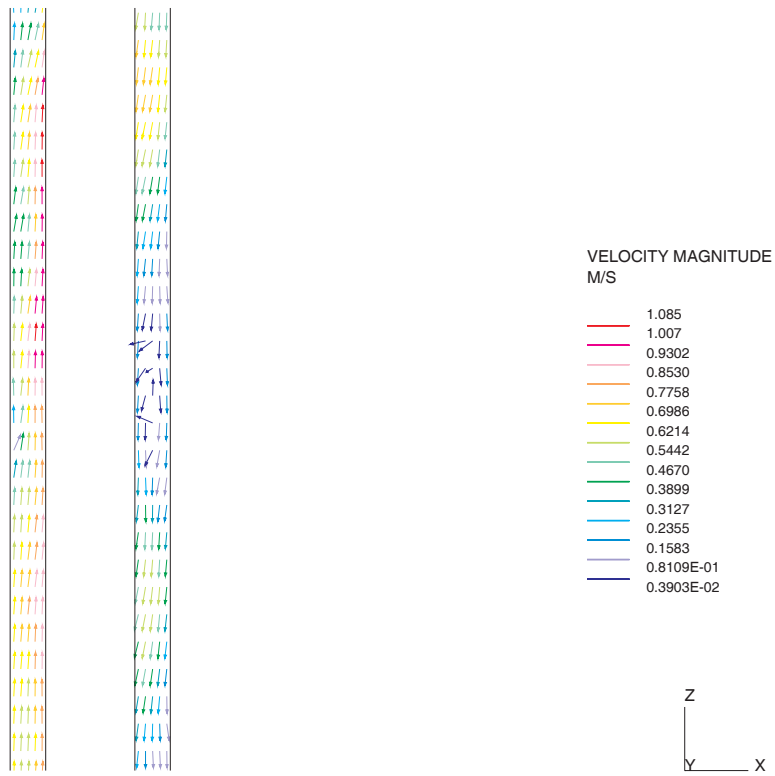
Figure 24. Air-flow in the "NSTF" cavity
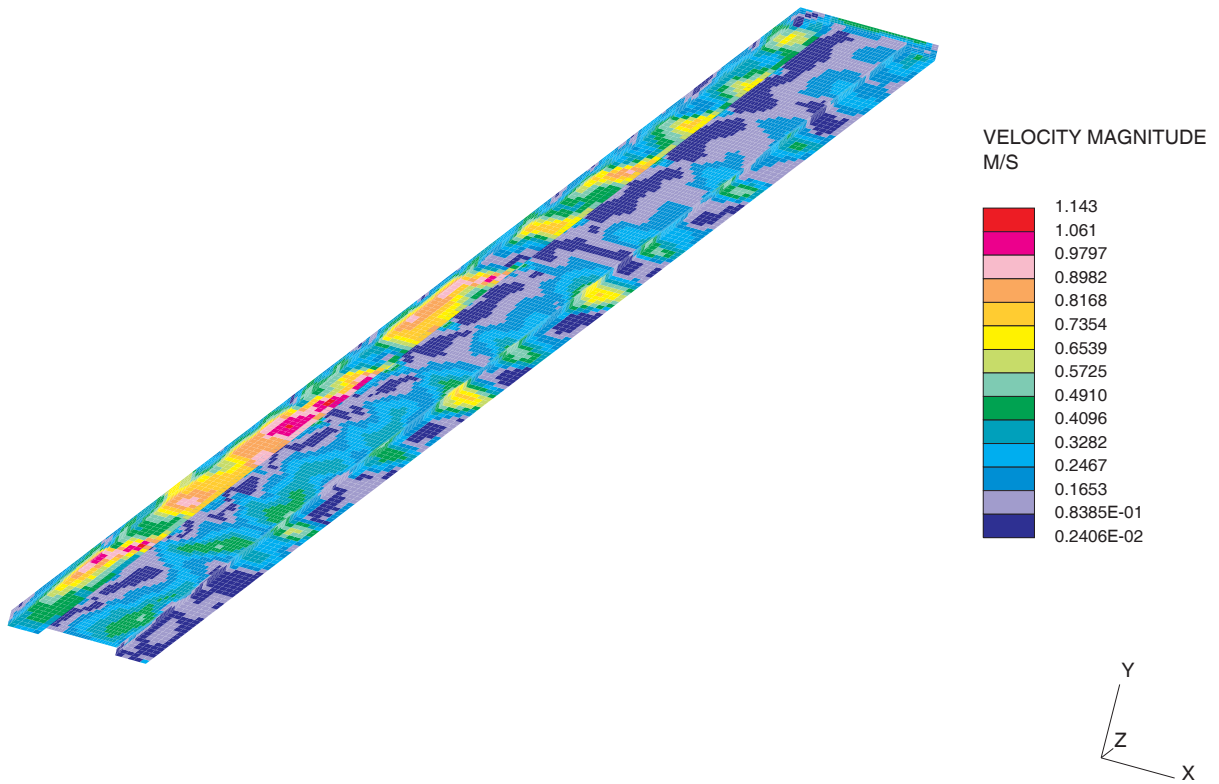
Figure 25. Velocity distribution in the "NSTF" cavity (laminar flow)
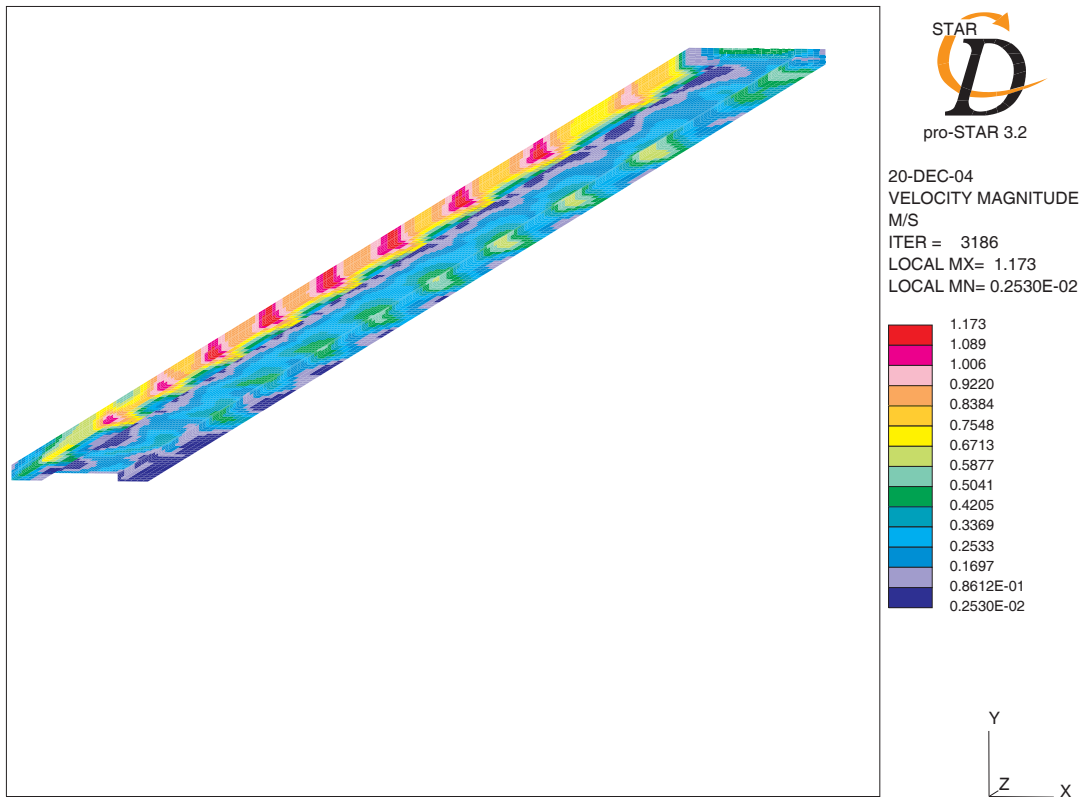
Figure 26. Velocity distribution in the "NSTF" cavity (k-ε model)

VELOCITY MAGNITUDE
M/S

	0.8125
	0.7547
	0.6969
	0.6391
	0.5813
	0.5235
	0.4657
	0.4079
	0.3501
	0.2923
	0.2345
	0.1767
	0.1189
	0.6112E-01
	0.3316E-02
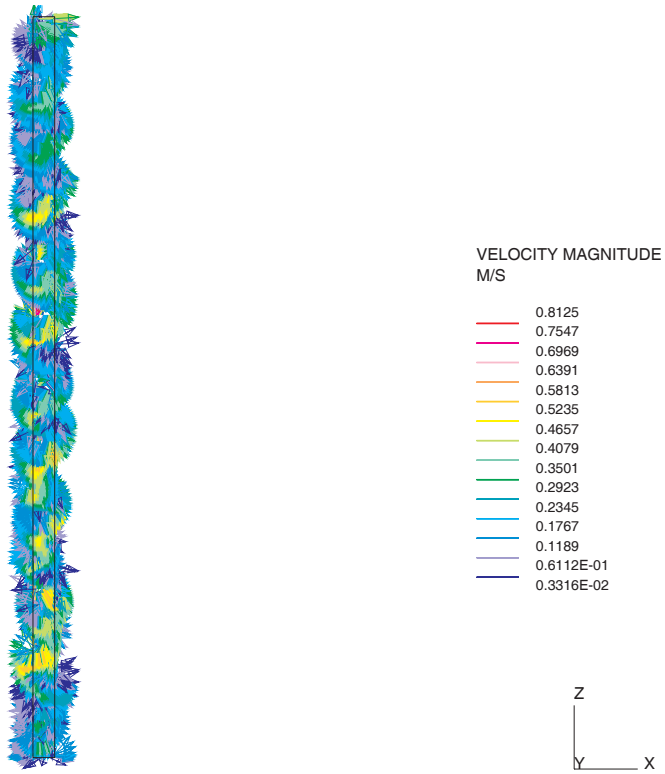
Figure 27. Velocity distribution in the gap between tubes
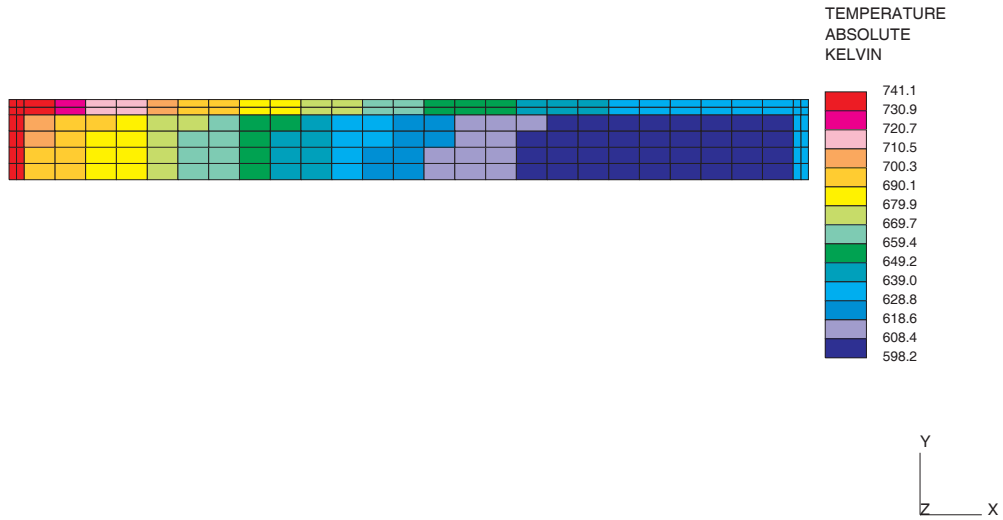
Figure 28.   Temperature distribution at 14.9 m (Uniform reactor vessel temperature of 560 °C)
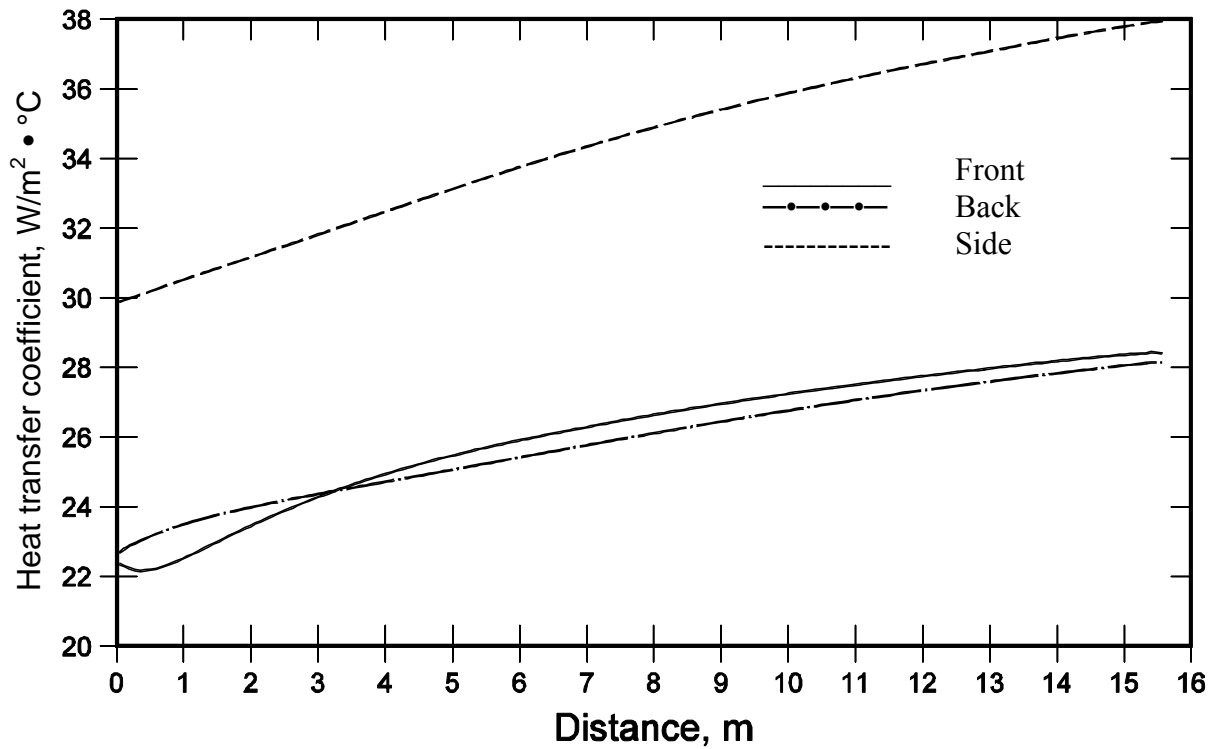
Figure 29. Heat transfer coefficient (uniform reactor vessel temperature 560 °C).

HEAT TRANSFER COEF.
W/(M**2 K)

37.82
37.12
36.42
35.72
35.03
34.33
33.63
32.93
32.23
31.53
30.83
30.14
29.44
28.74
28.04
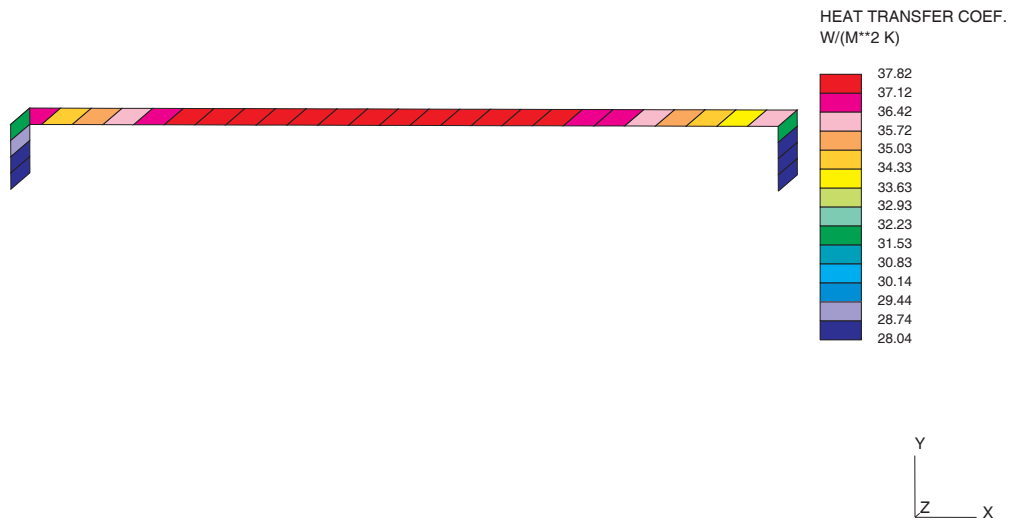
Figure 30. Heat transfer coefficient around the tube at 14.9 m (uniform reactor vessel temperature of 560 °C)
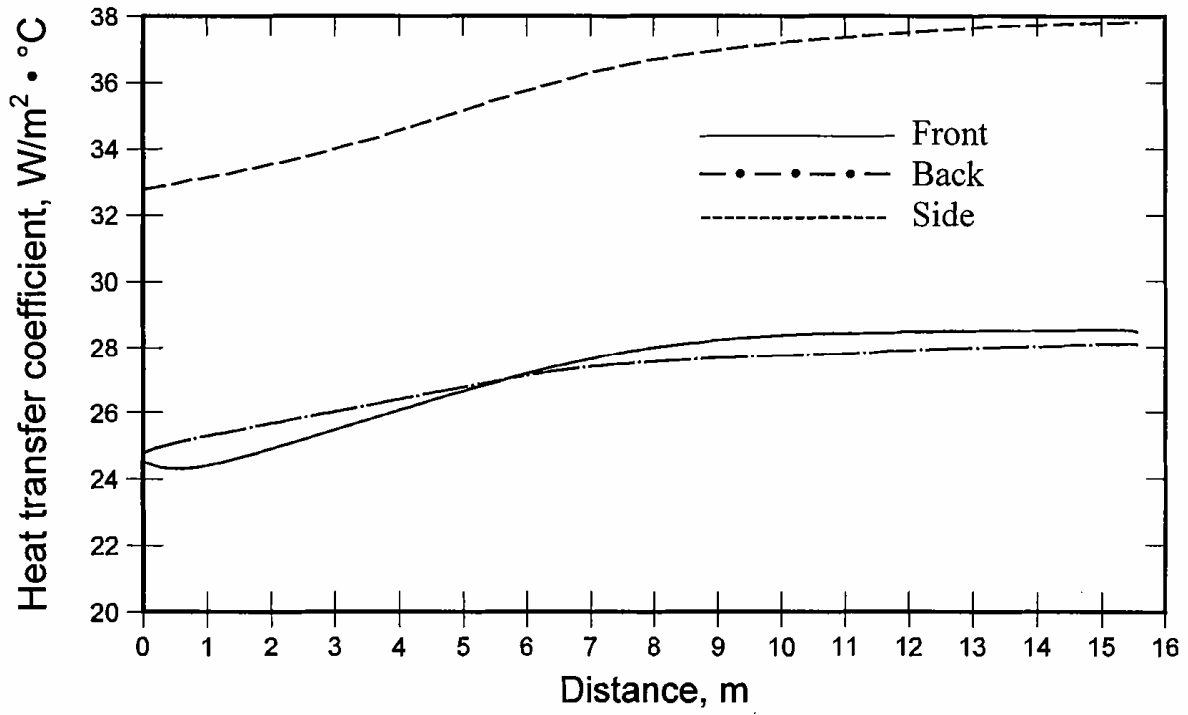
Figure 31. Heat transfer coefficient (non-uniform reactor vessel temperature - peak of 560 °C).
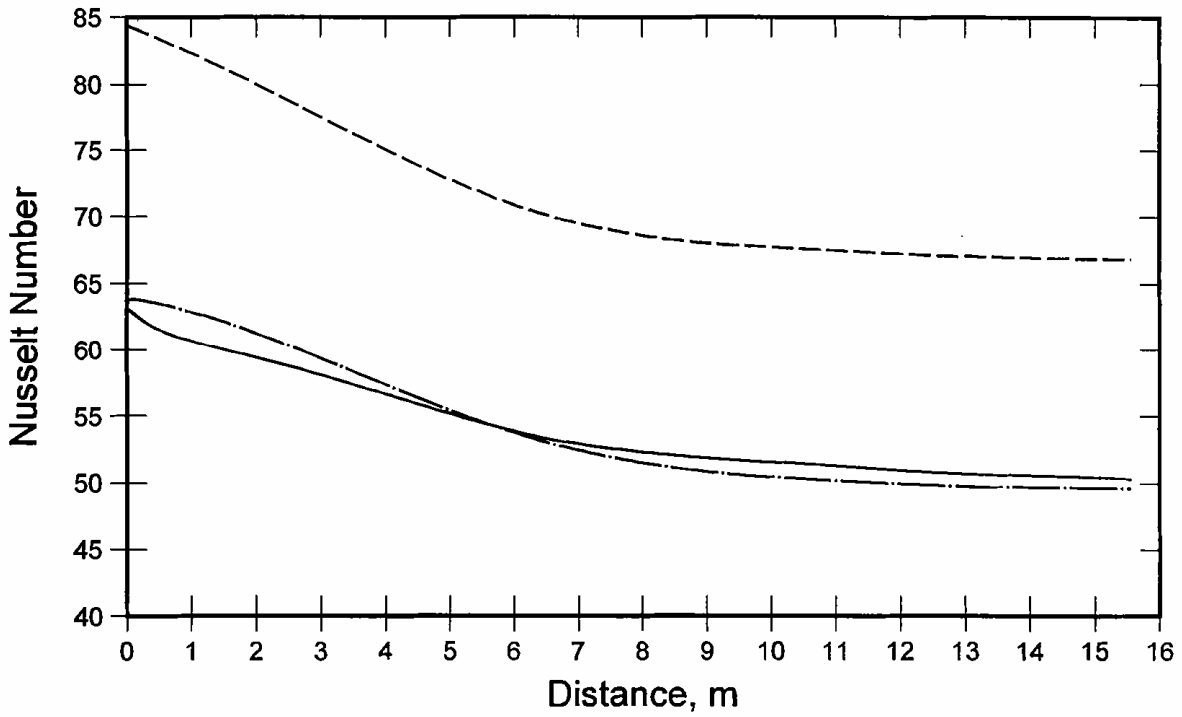
Figure 32. Nusselt number (non-uniform reactor vessel temperature - peak of 560 °C).

41
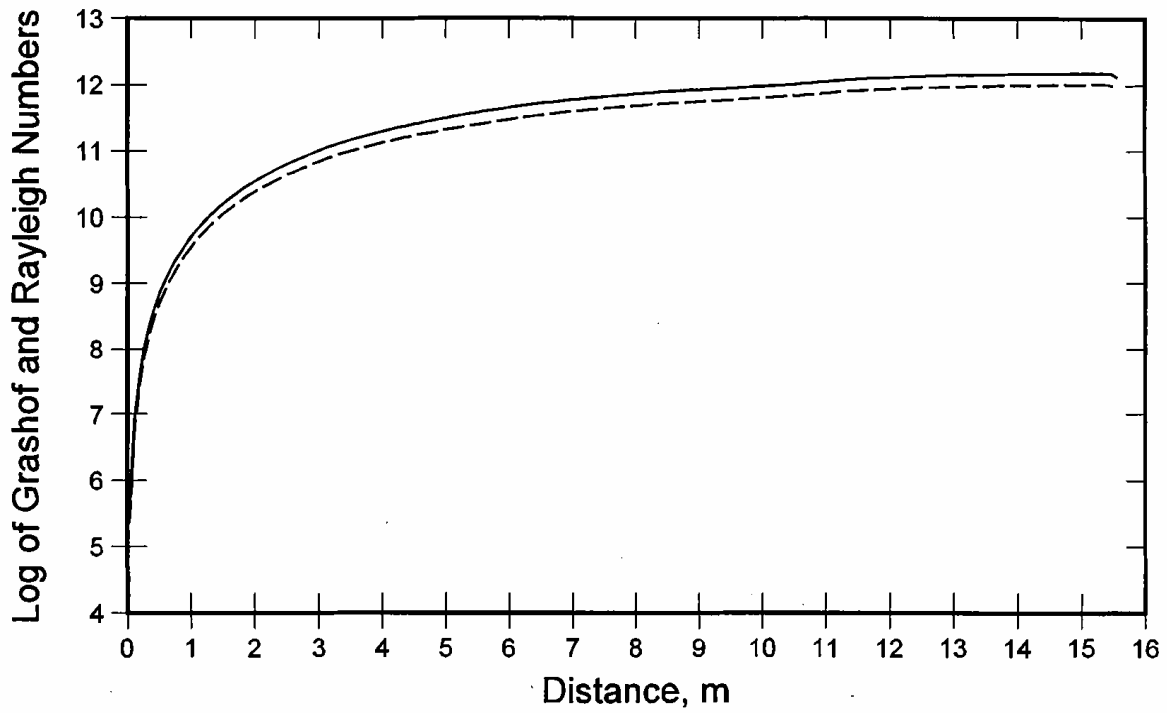
Figure 33. Grashof and Rayleigh numbers along the axis of the front tube wall (non-uniform reactor vessel temperature - peak of 560 °C).
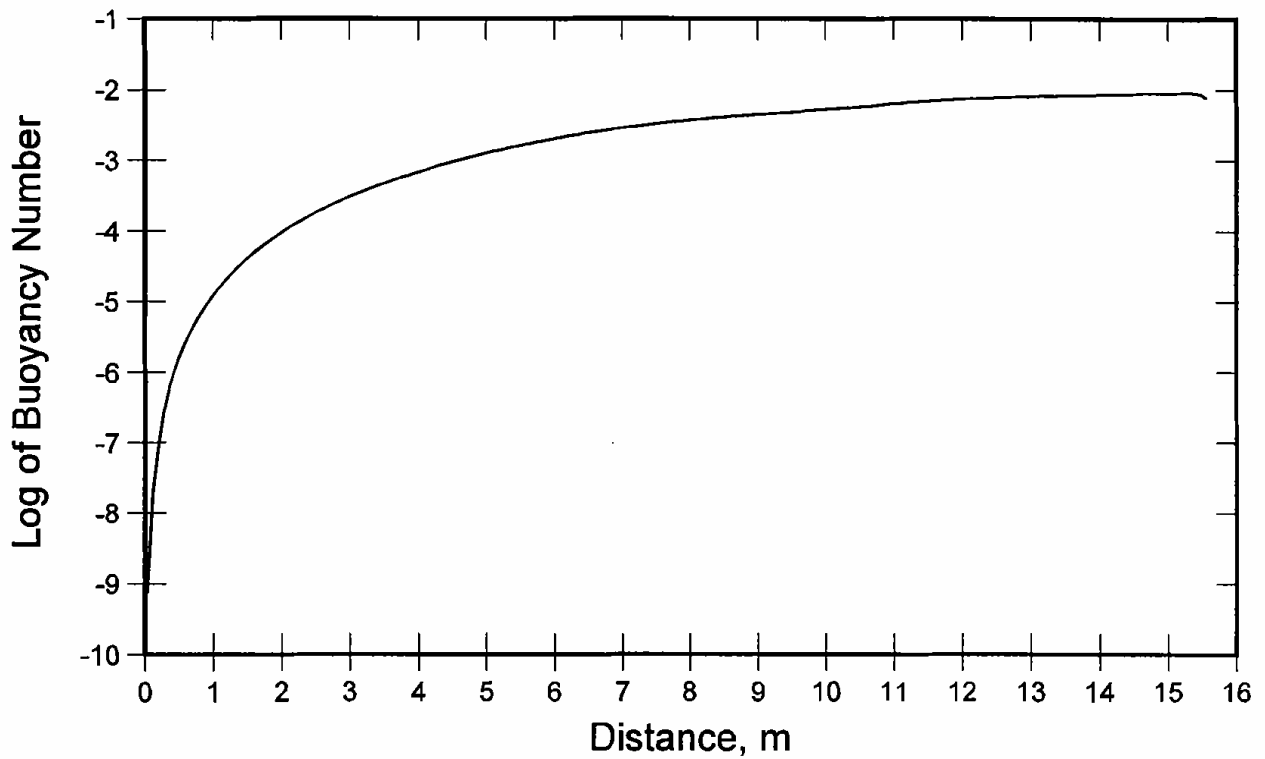
Figure 34. Buoyancy number along the axis of the front tube wall (non-uniform reactor vessel temperature - peak of 560 °C).

42
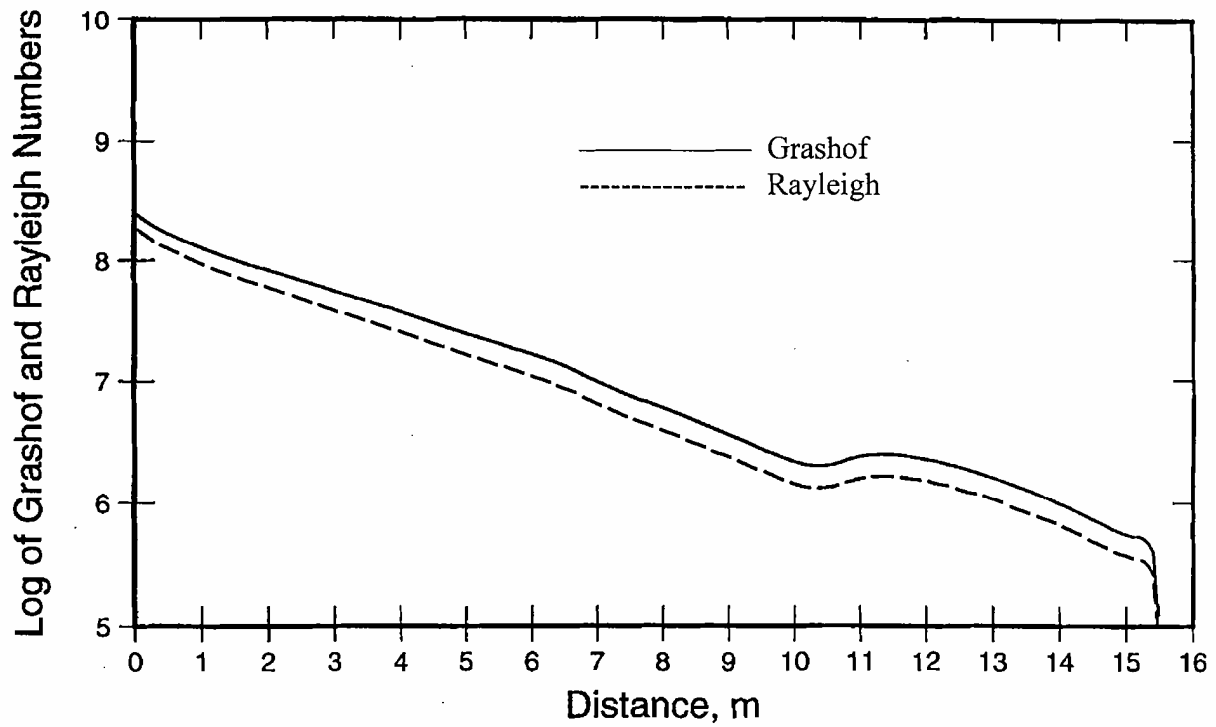
Figure 35. Grashof and Rayleigh numbers: front wall of RCCS tube (based on hydraulic diameter; variable reactor vessel temperature, peak of 560 °C).
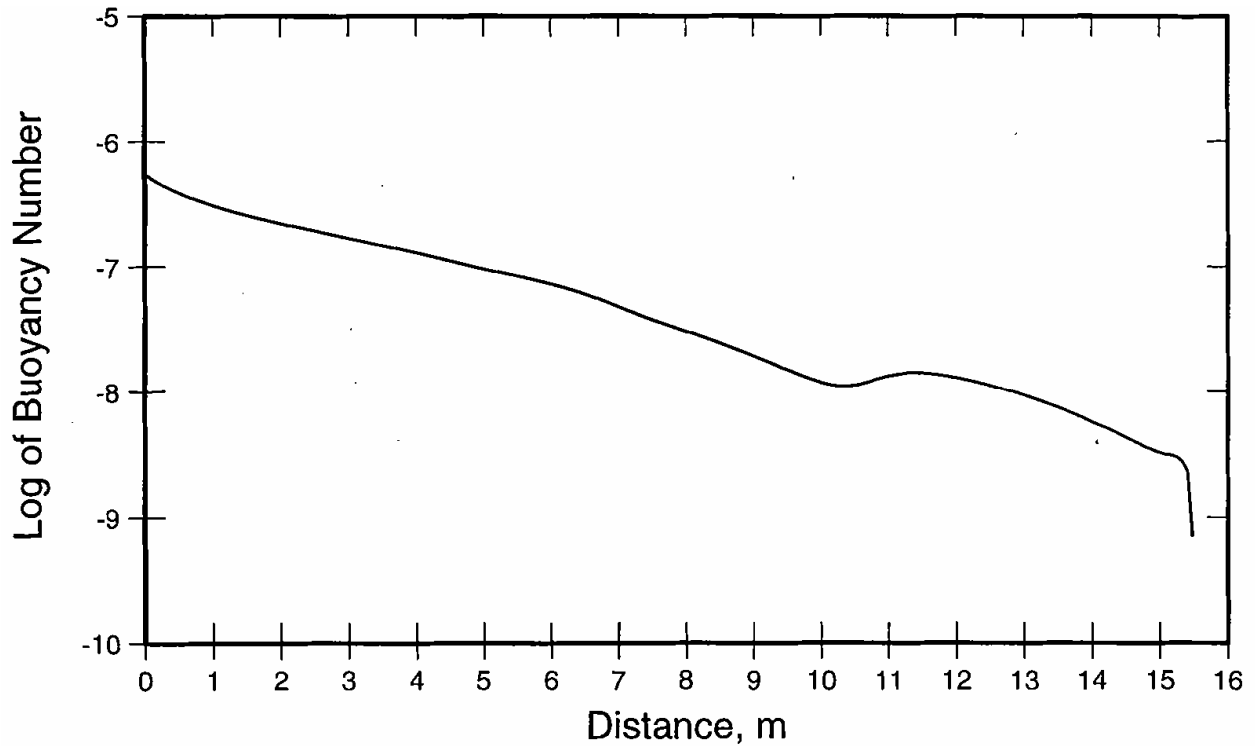
Figure 36. Buoyancy number; front wall of RCCS tube (based on hydraulic diameter; variable reactor vessel temperature, peak of 560 °C).
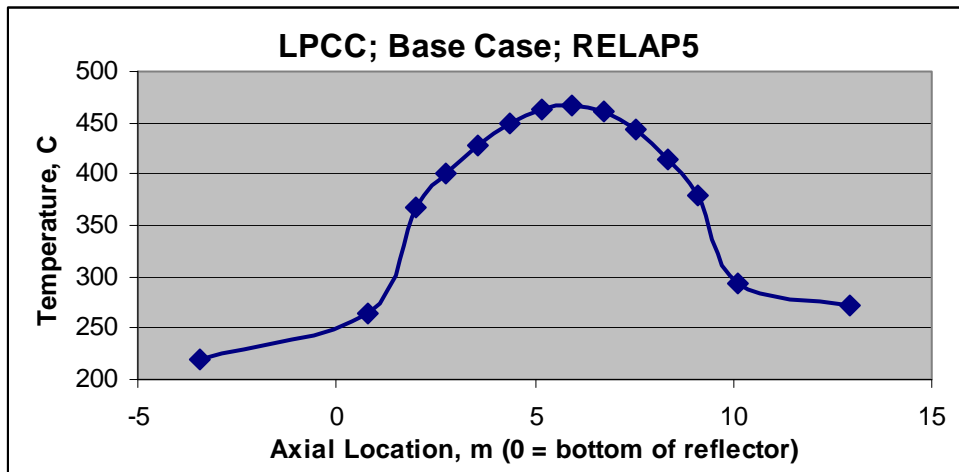
Figure 37. Reactor vessel temperature distribution (VHTR1000)
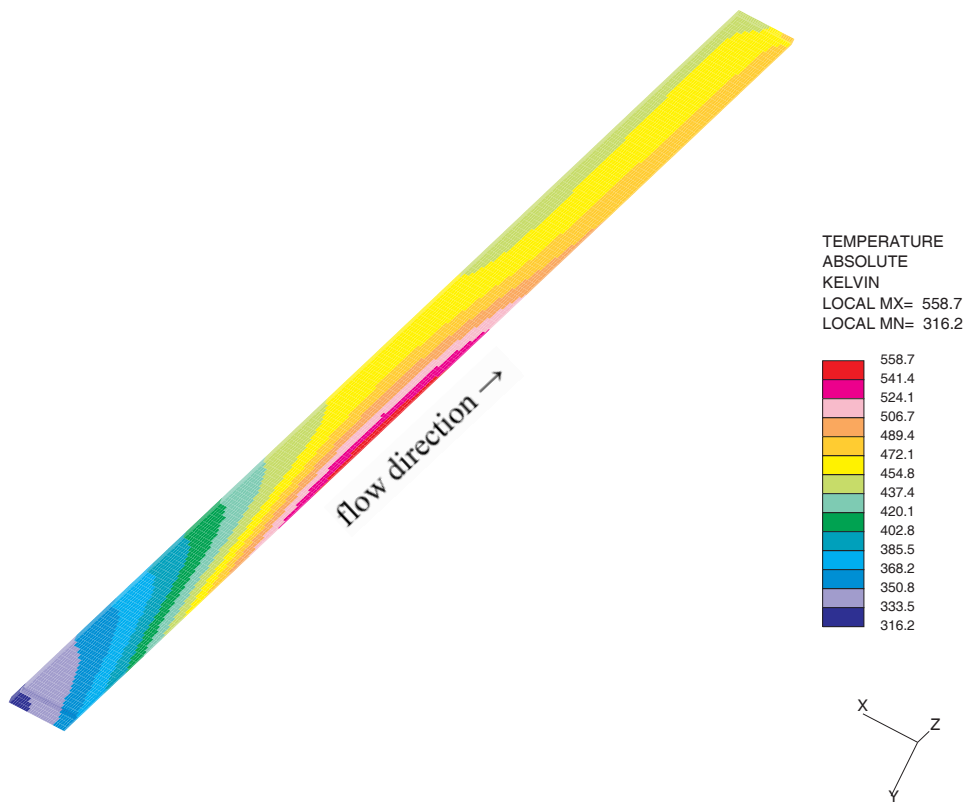
Figure 38. Air temperature distribution along the RCCS tube (VHTR1000)

TEMPERATURE
ABSOLUTE
KELVIN
LOCAL MX= 546.3
LOCAL MN= 357.0

546.3
532.8
519.3
505.8
492.2
478.7
465.2
451.7
438.1
424.6
411.1
397.6
384.0
370.5
357.0
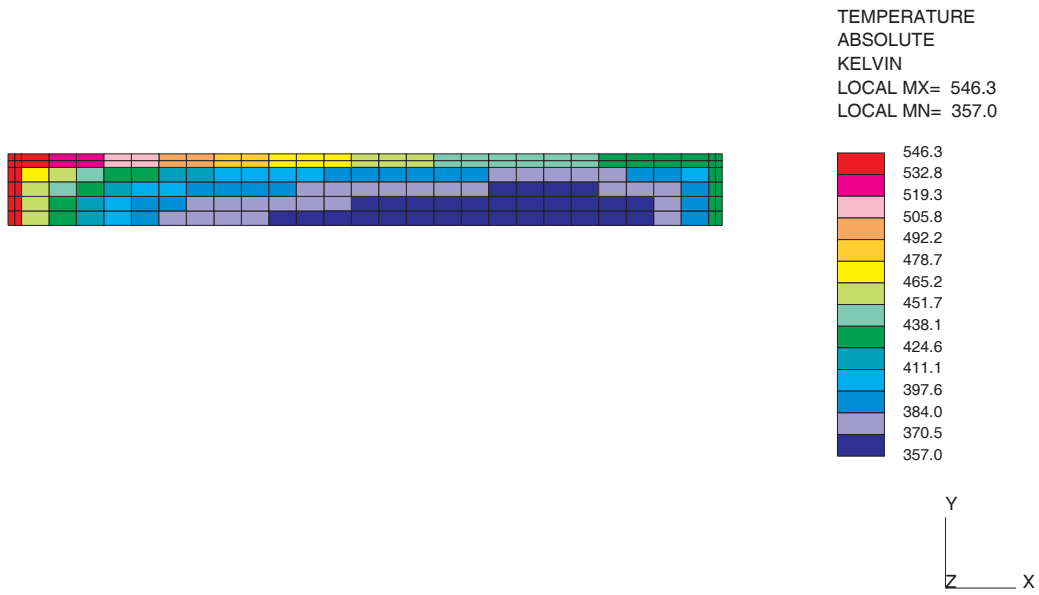
Figure 39. Tube and air temperature distribution at 5.3 m (VHTR1000)
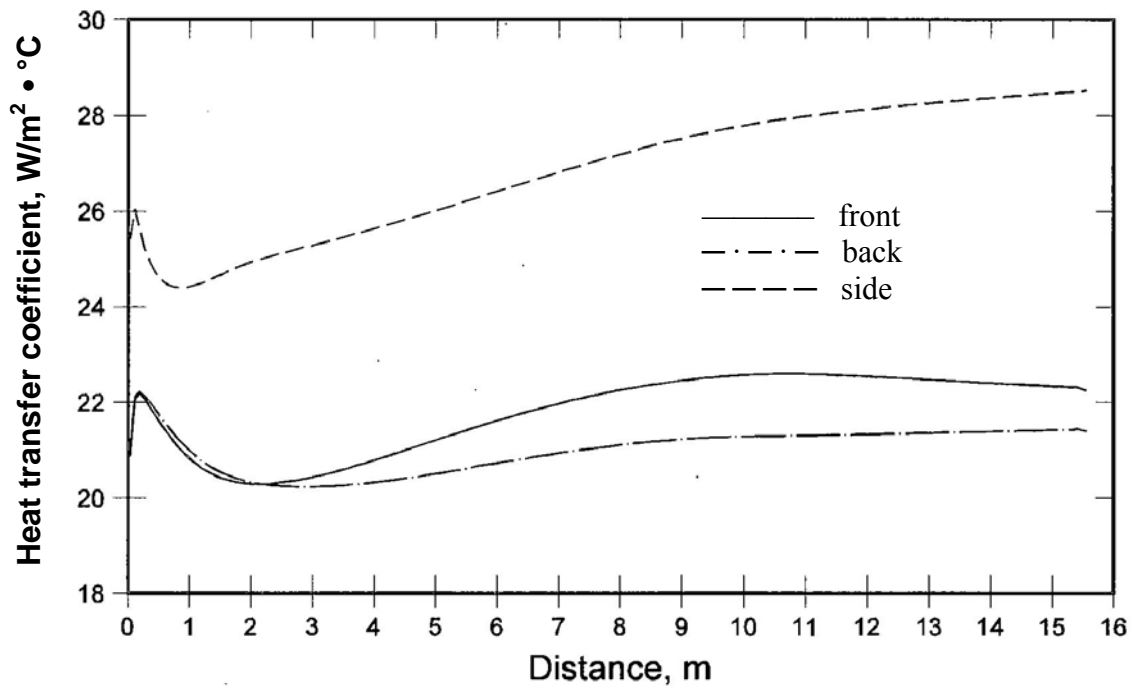
Figure 40. Heat transfer coefficients (VHTR1000)
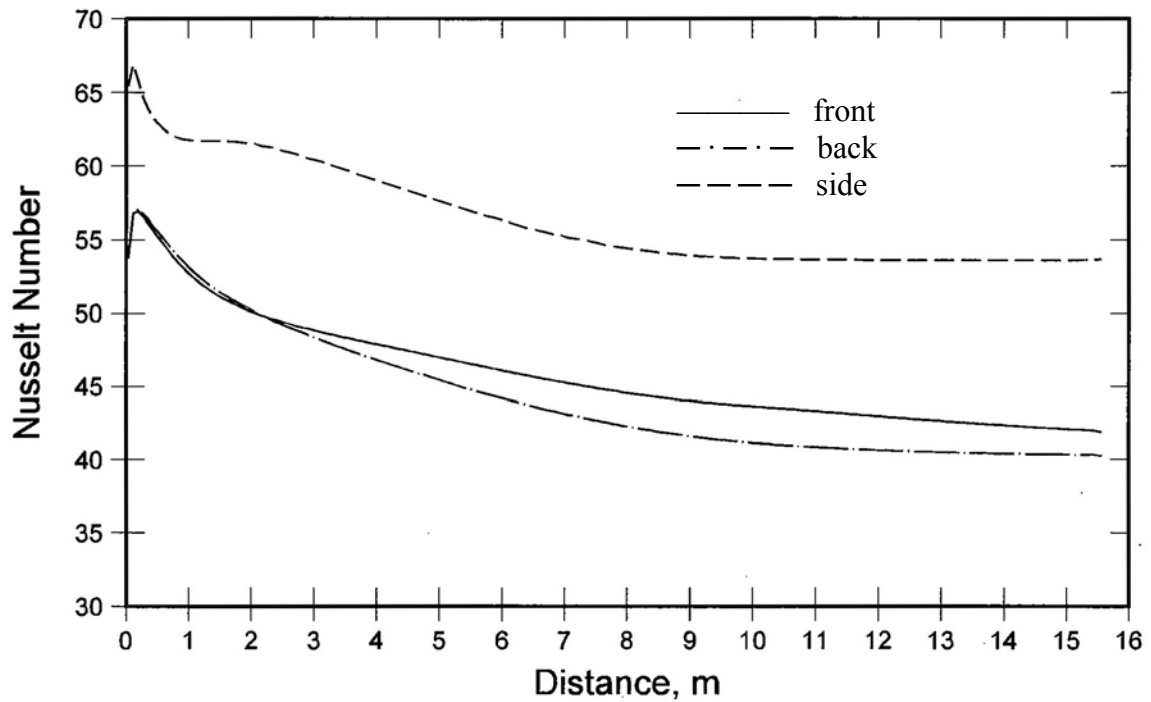
Figure 41. Nusselt number vs. tube height (VHTR1000)
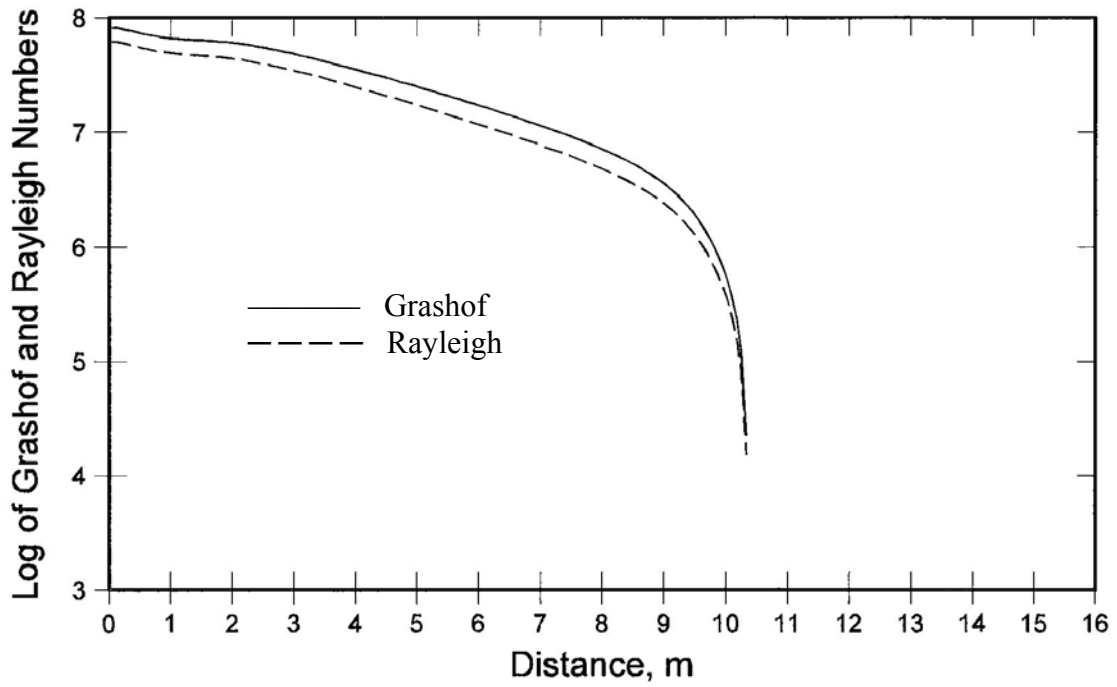
Figure 42. Grashof and Rayleigh numbers vs. tube height
(VHTR1000)
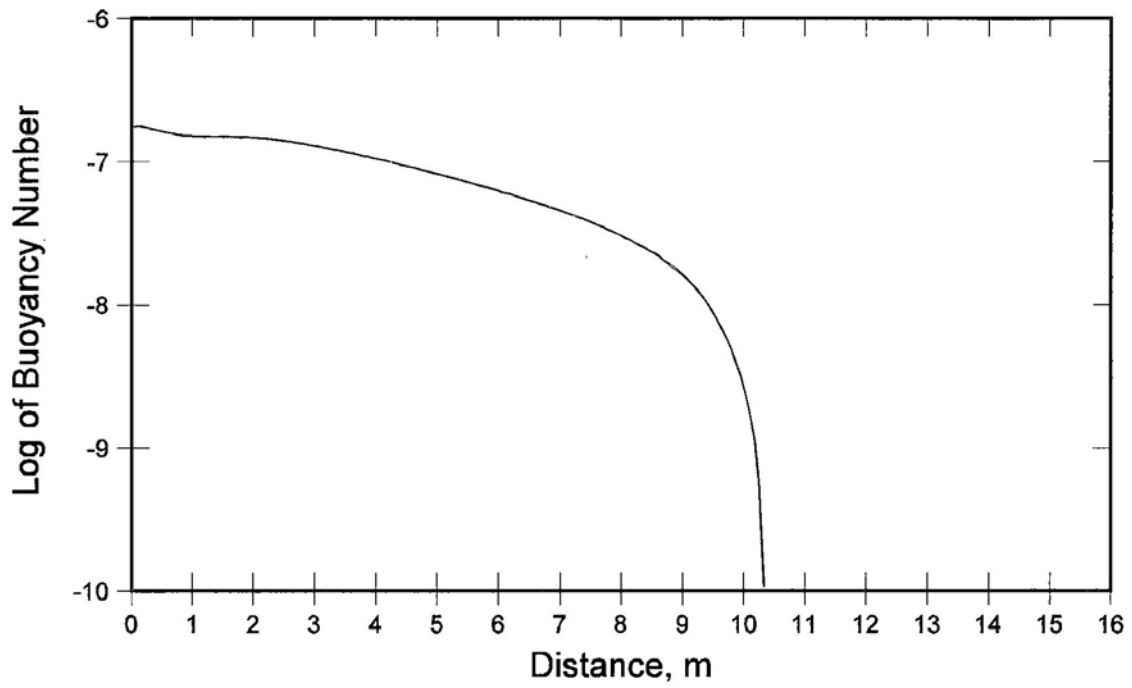
Figure 43. Buoyancy number vs. tube height (VHTR1000)
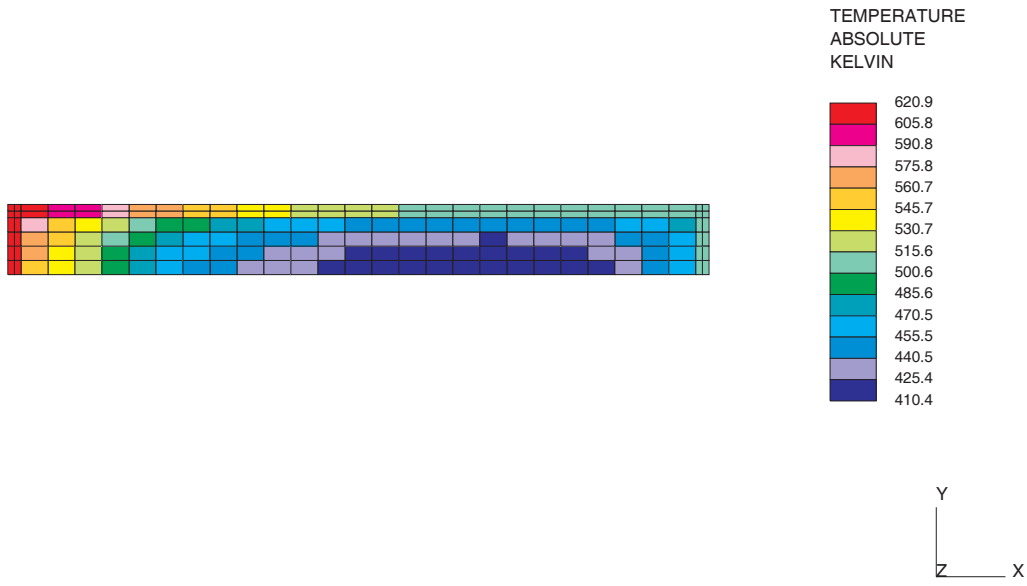
Figure 44. NSTF tube temperature distribution at 6.7 m (heated wall temperature of 480 °C).
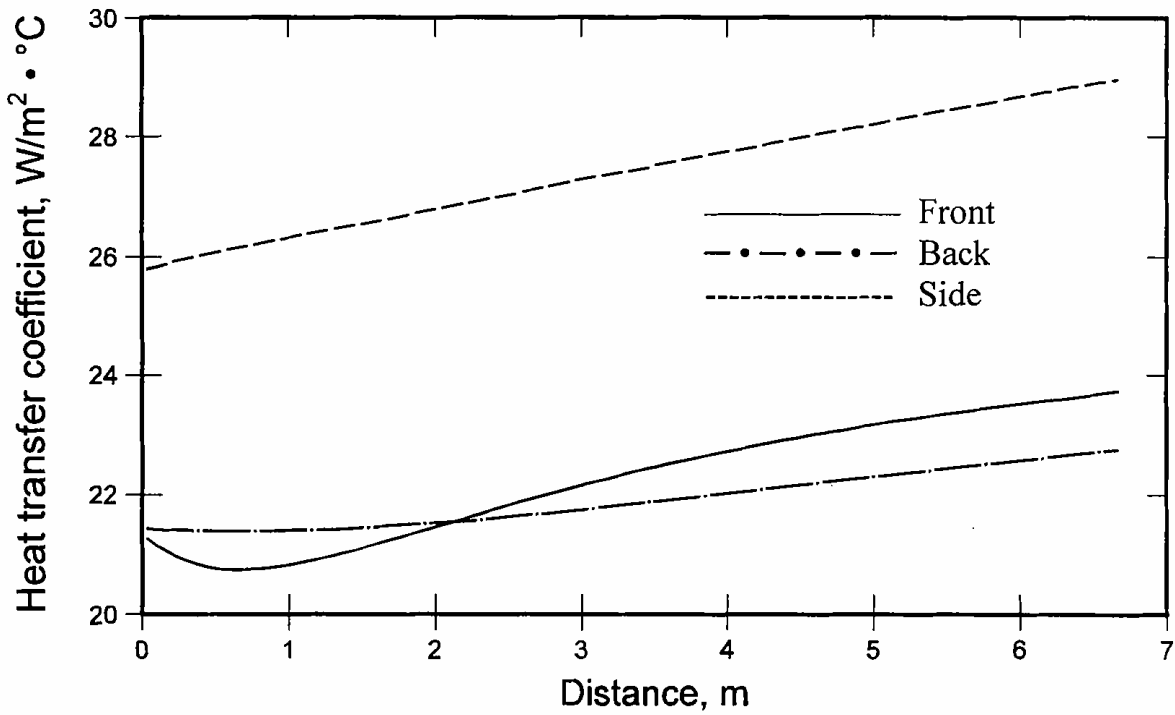
Figure 45. NSTF heat transfer coefficient (heated wall temperature of 480 °C)
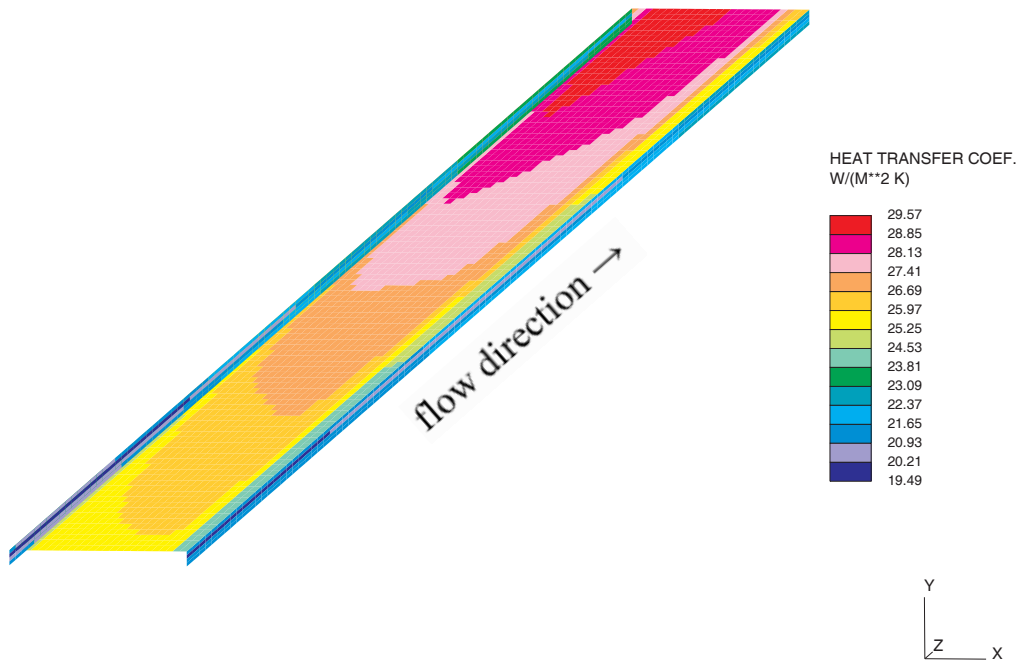
Figure 46. Variation of heat transfer coefficient around the tube walls (NSTF heated wall temperature of 480 °C).
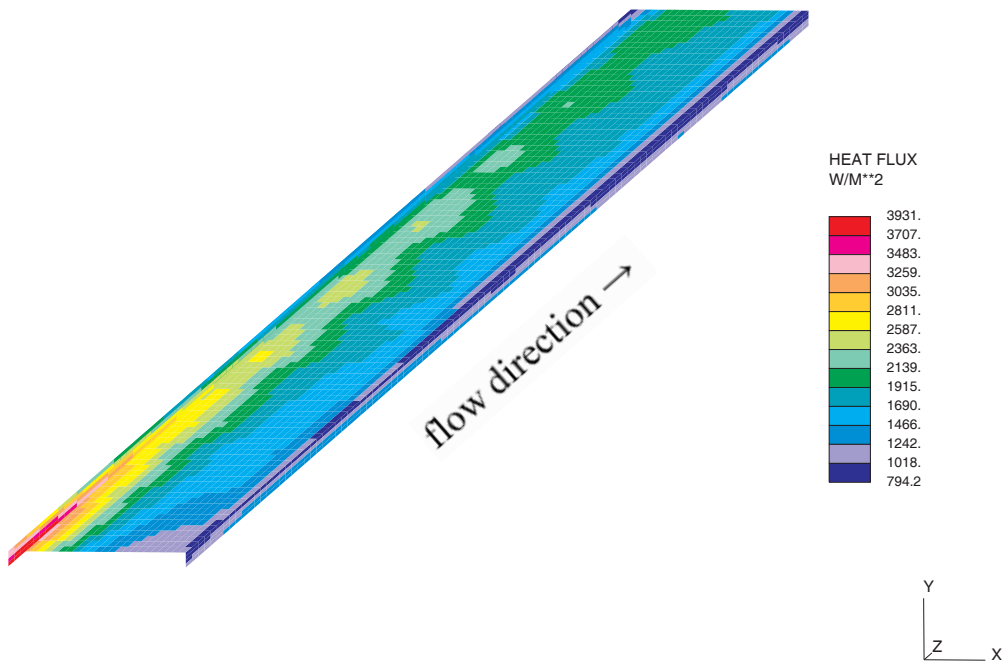
Figure 47. Variation of heat flux around the tube walls (NSTF heated wall temperature of 480 °C).
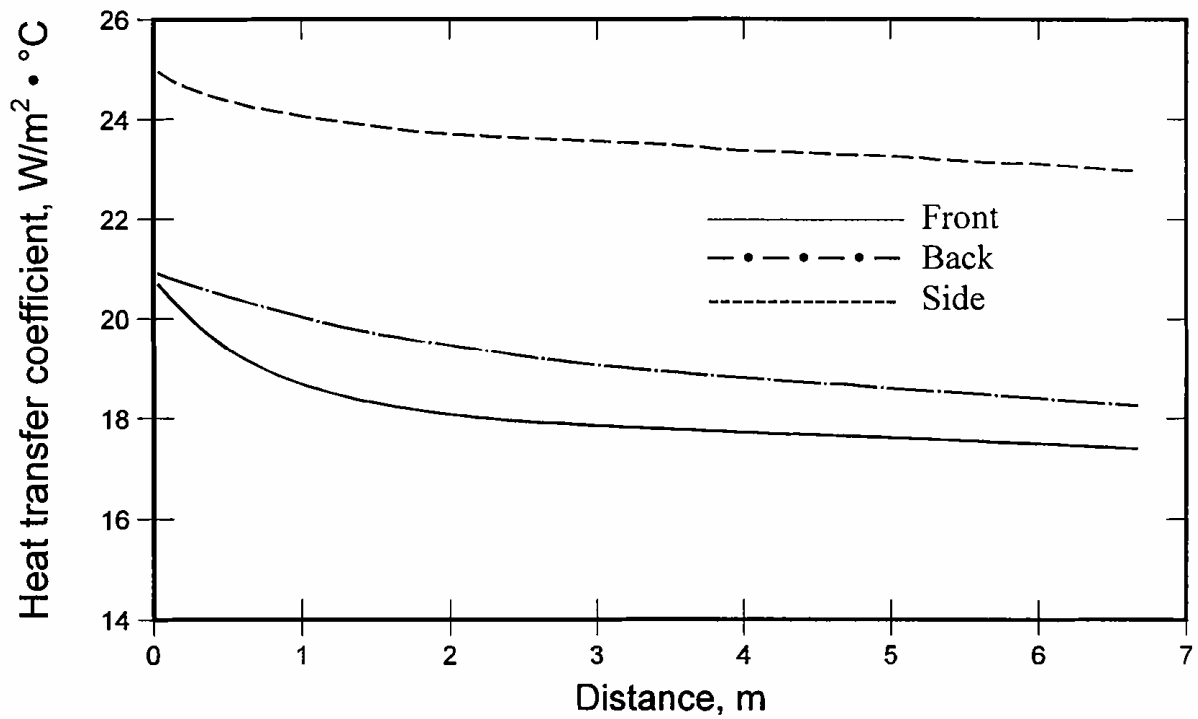
Figure 48. Heat transfer coefficient for a constant air thermal conductivity (NSTF heated wall temperature of 480 °C).
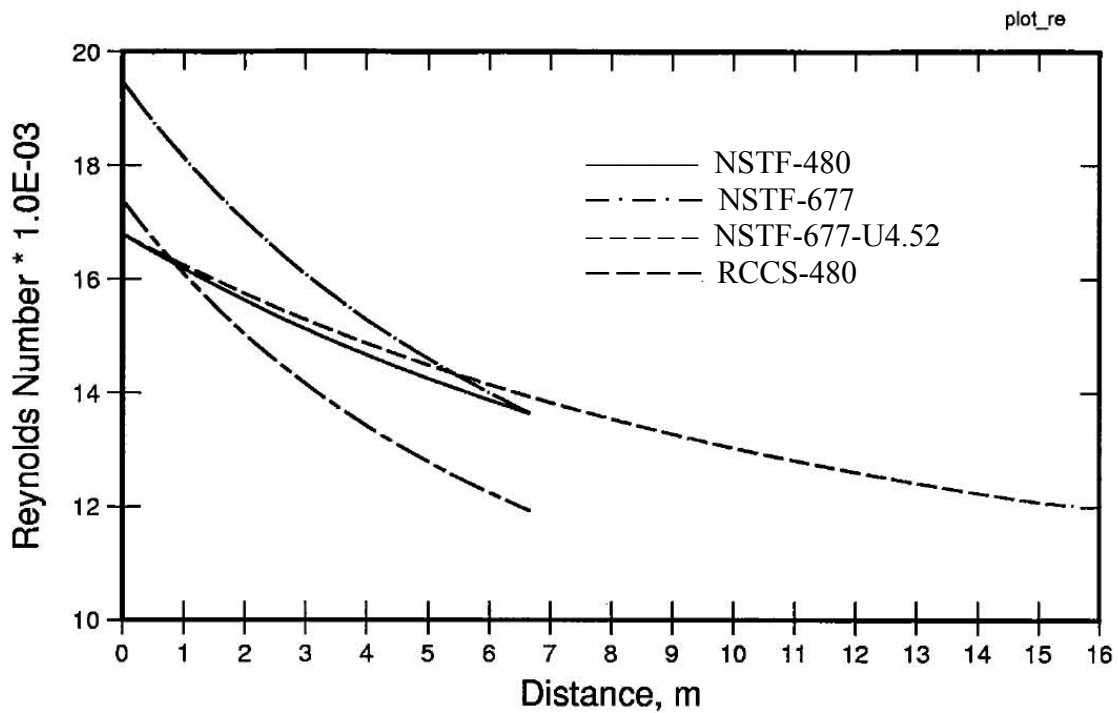
Figure 49. Reynolds number versus tube height.
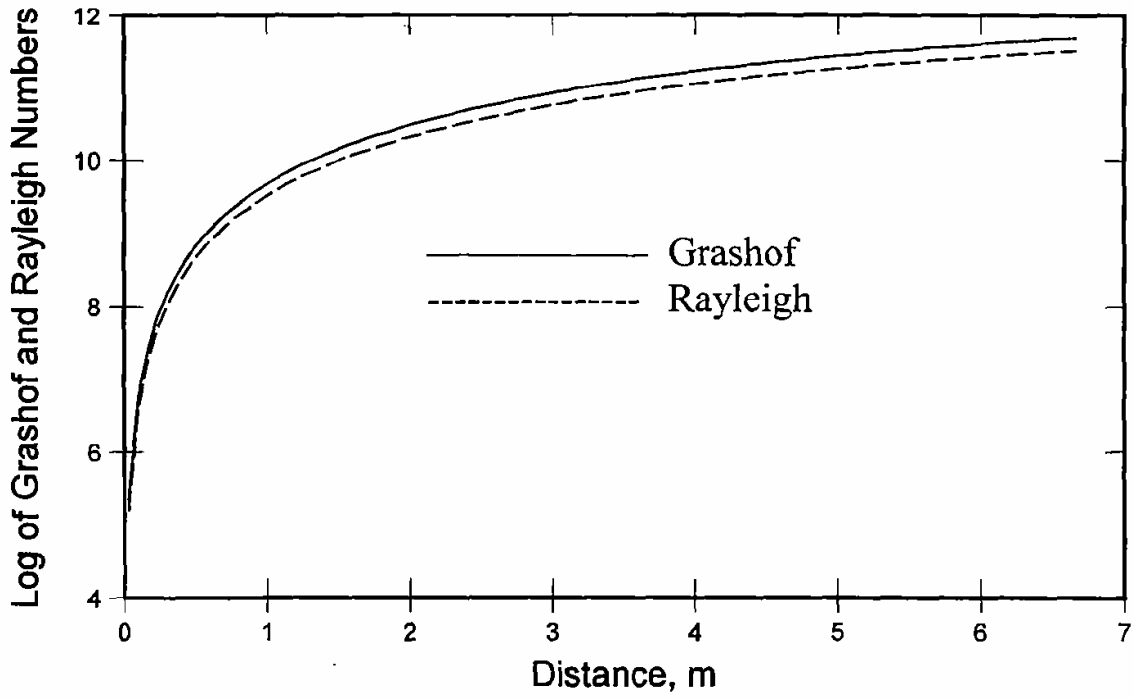
Figure 50. Grashof and Rayleigh numbers versus tube height (NSTF heated wall temperature of 480 °C).
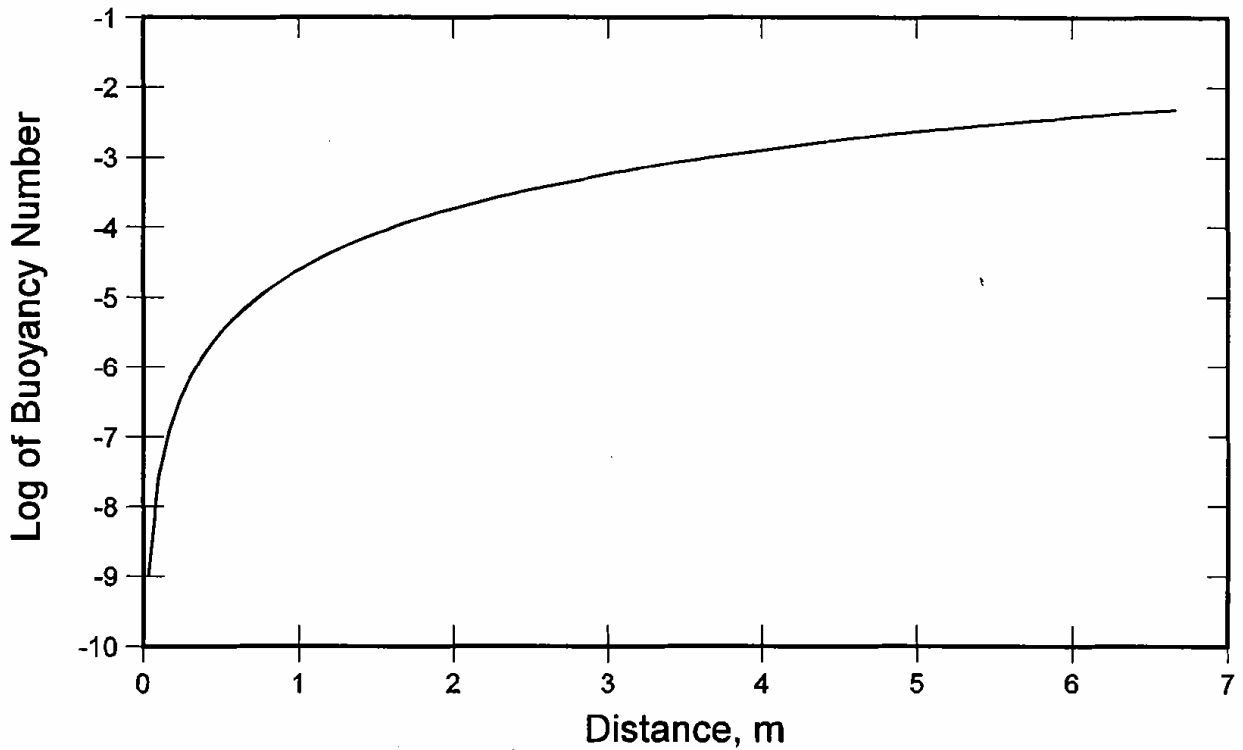
Figure 51. Buoyancy number versus tube height (NSTF heated wall temperature of 480 °C).
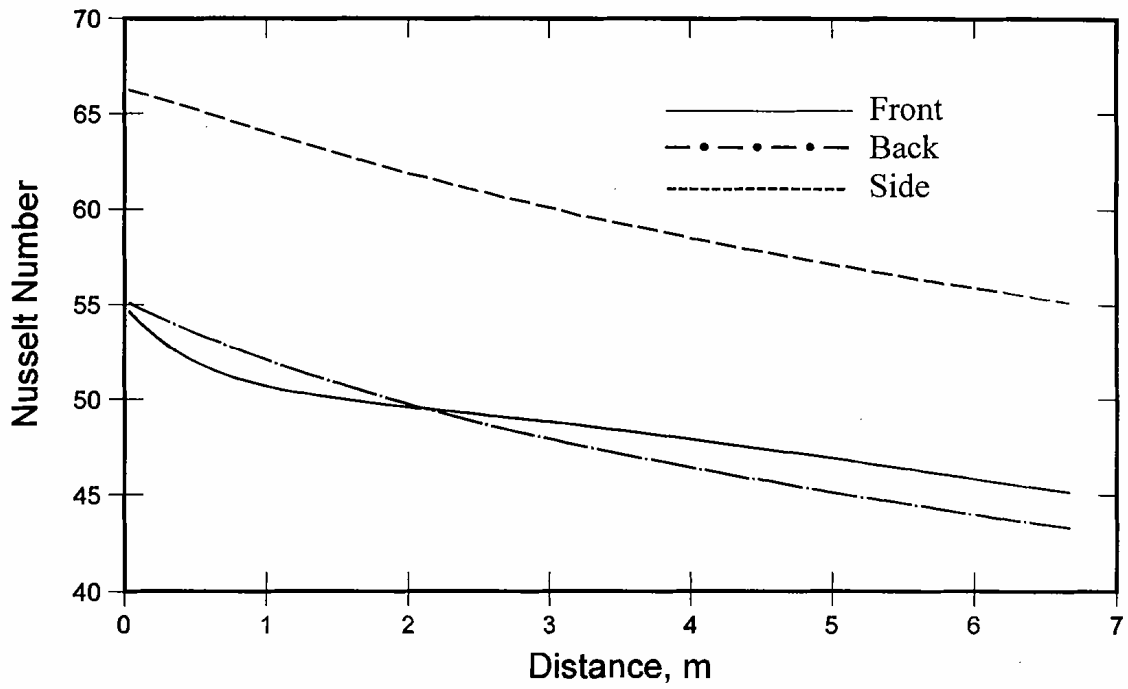
Figure 52. Nusselt number versus NSTF tube height (NSTF heated wall temperature of 480 °C).
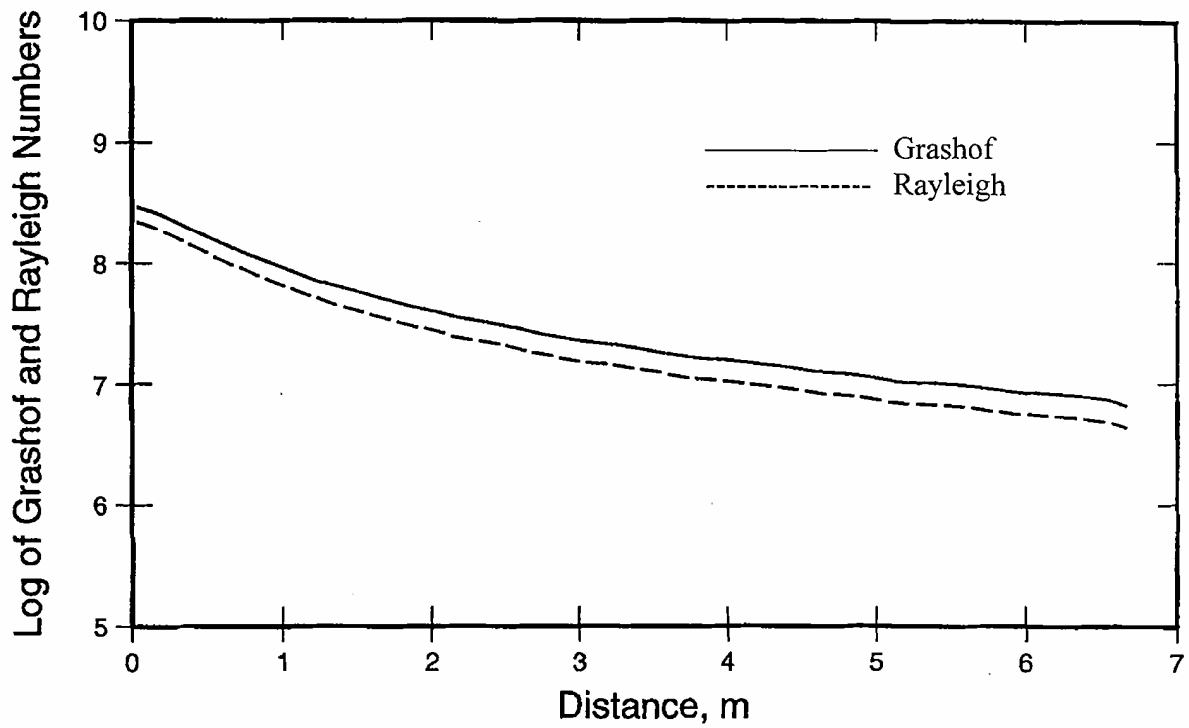
Figure 53. Grashof and Rayleigh numbers; front wall of NSTF tube (based on hydraulic diameter and heated wall temperature of 480 °C).
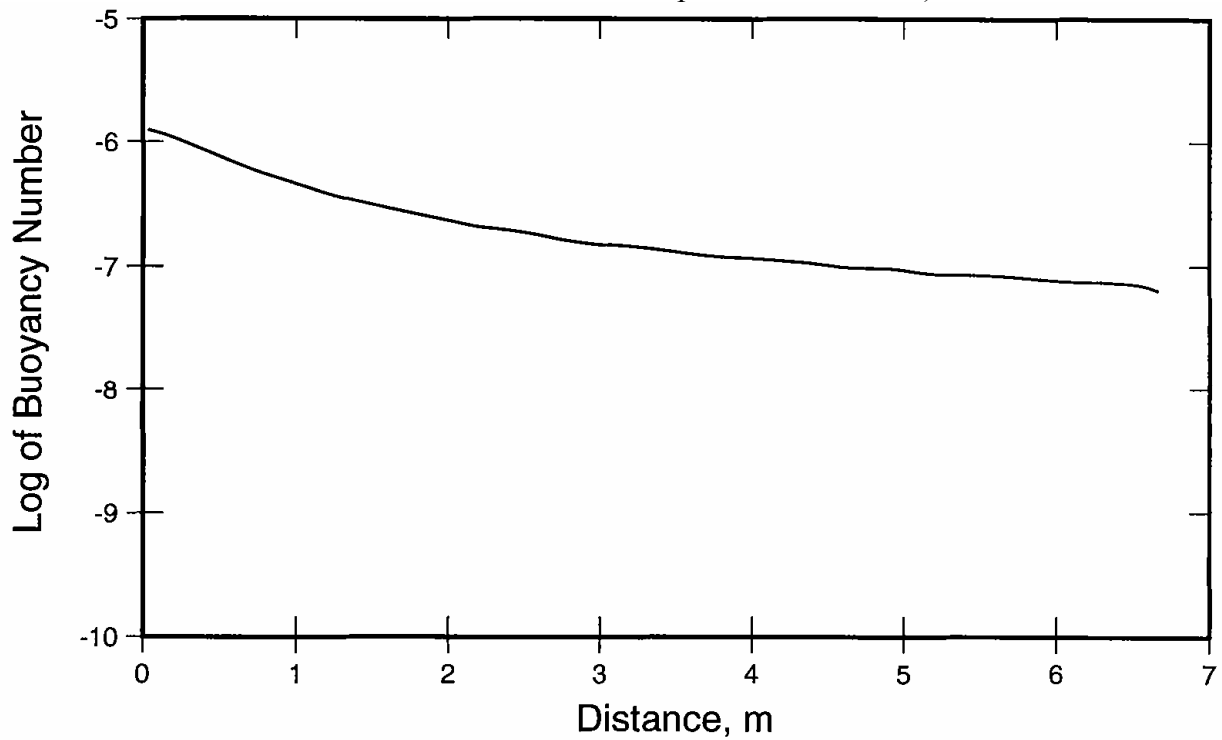
Figure 54. Buoyancy number; front wall of NSTF (based on hydraulic diameter and heated wall temperature: 480 °C).
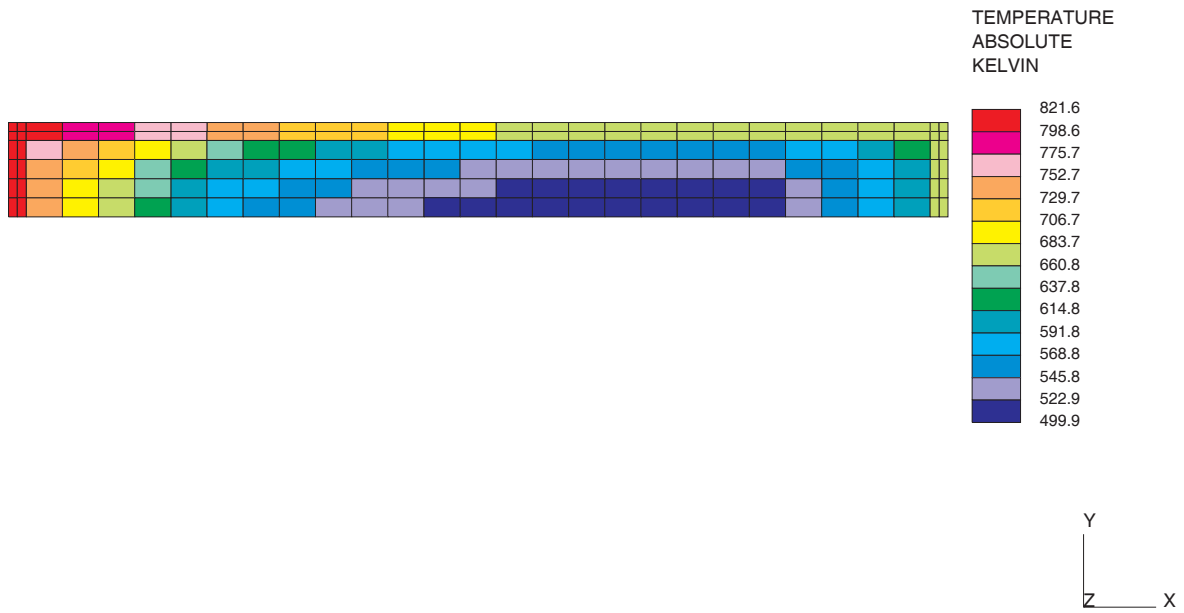
Figure 55. NSTF tube temperature distribution at 6.7 m (heated wall temperature of 677 °C).
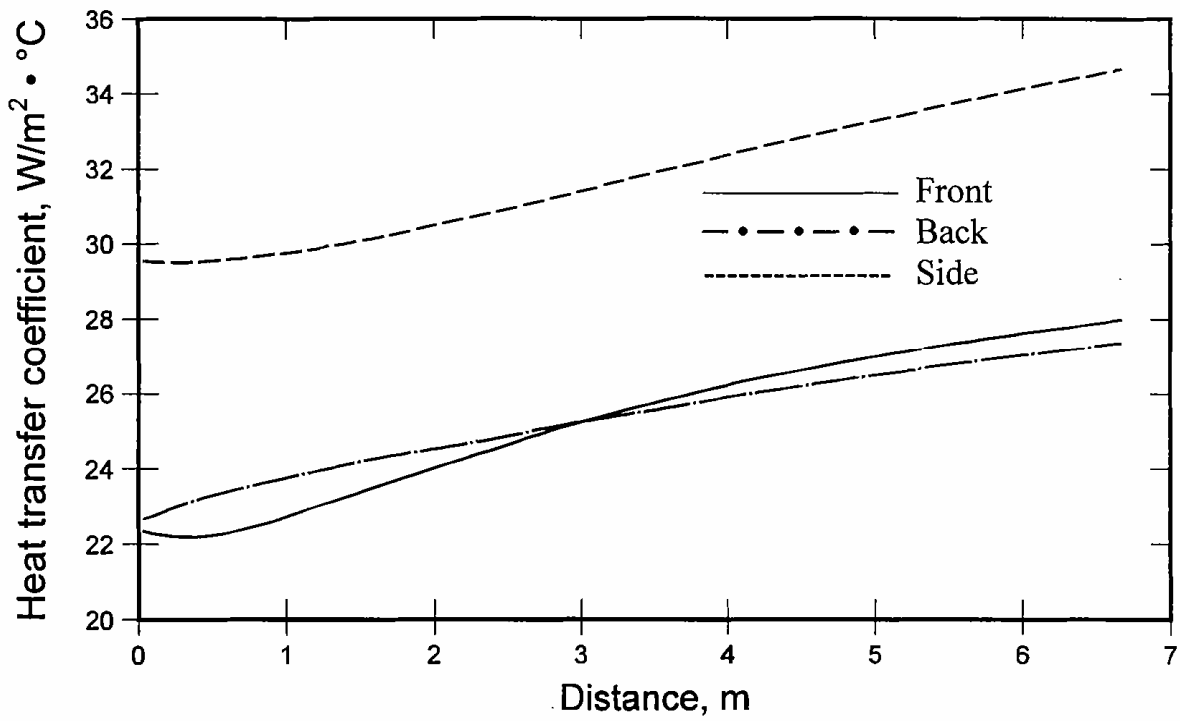
Figure 56. Heat transfer coefficient for an NSTF heated wall temperature of 677 °C.
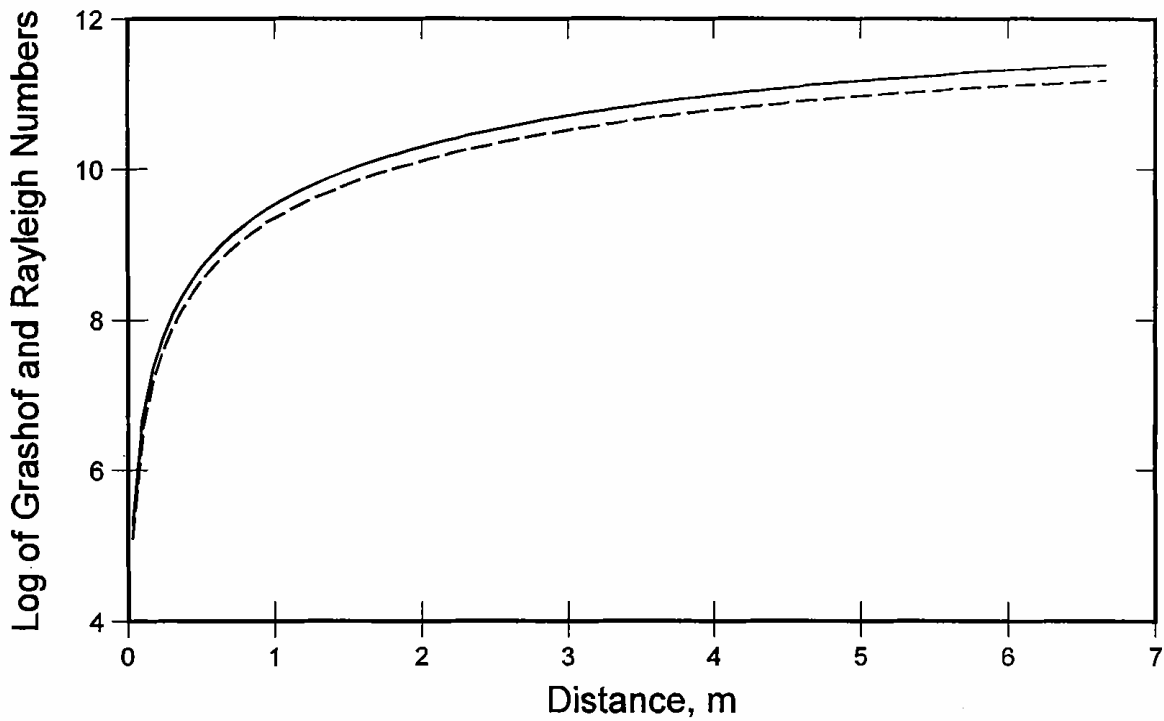
Figure 57. Grashof and Rayleigh numbers for an NSTF heated wall temperature of 677 °C.
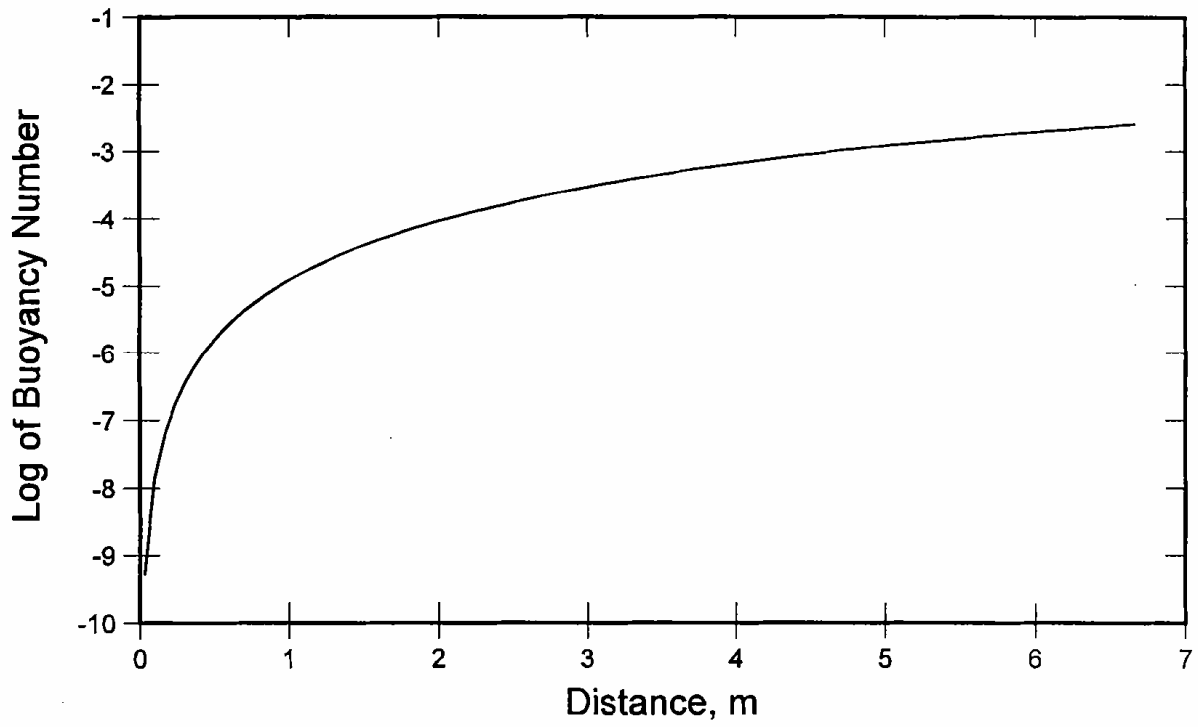
Figure 58. Buoyancy number (NSTF heated wall temperature of 677 °C).
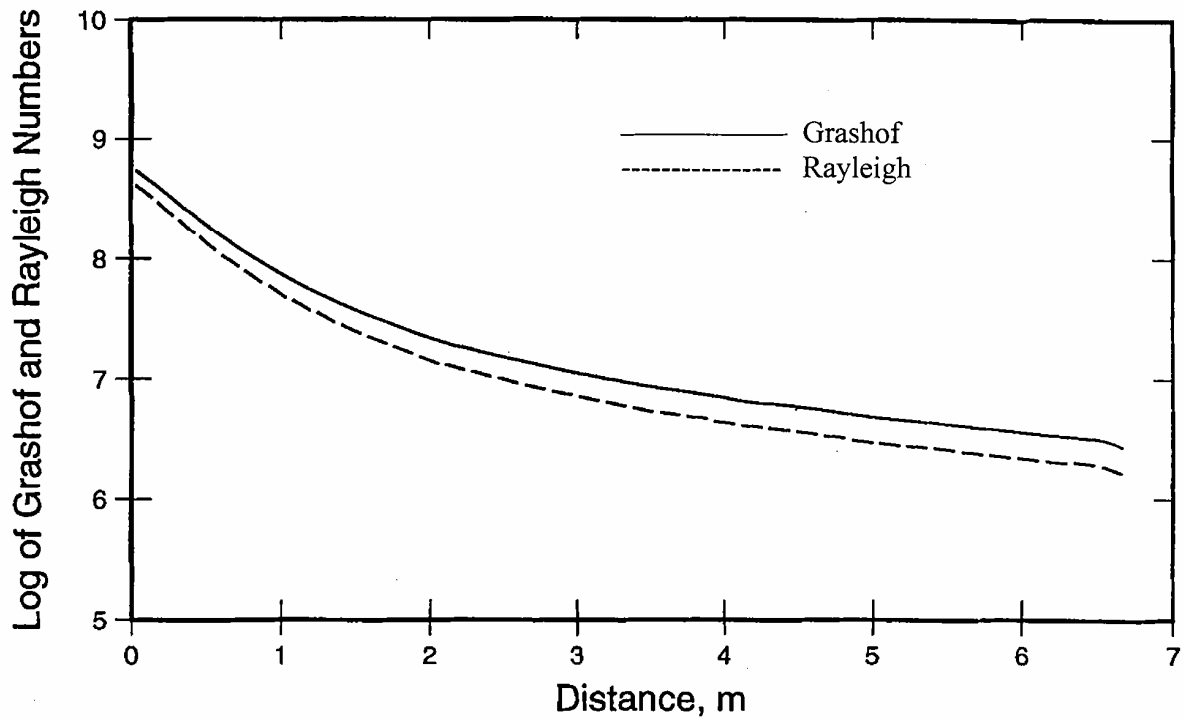
Figure 59. Grashof and Rayleigh numbers; front wall of NSTF tube (based on hydraulic diameter and heated wall temperature of 677 °C).
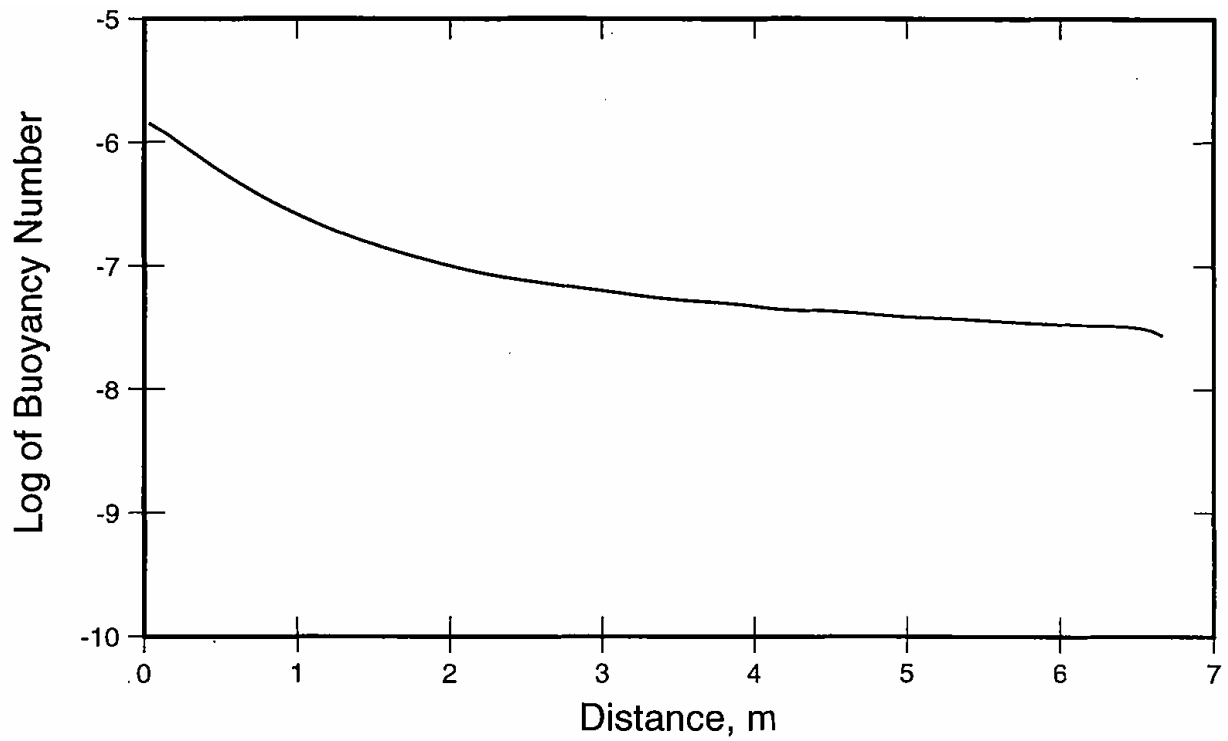
Figure 60. Buoyancy number; front wall of NSTF tube (based on hydraulic diameter and heated wall temperature of 677 °C).
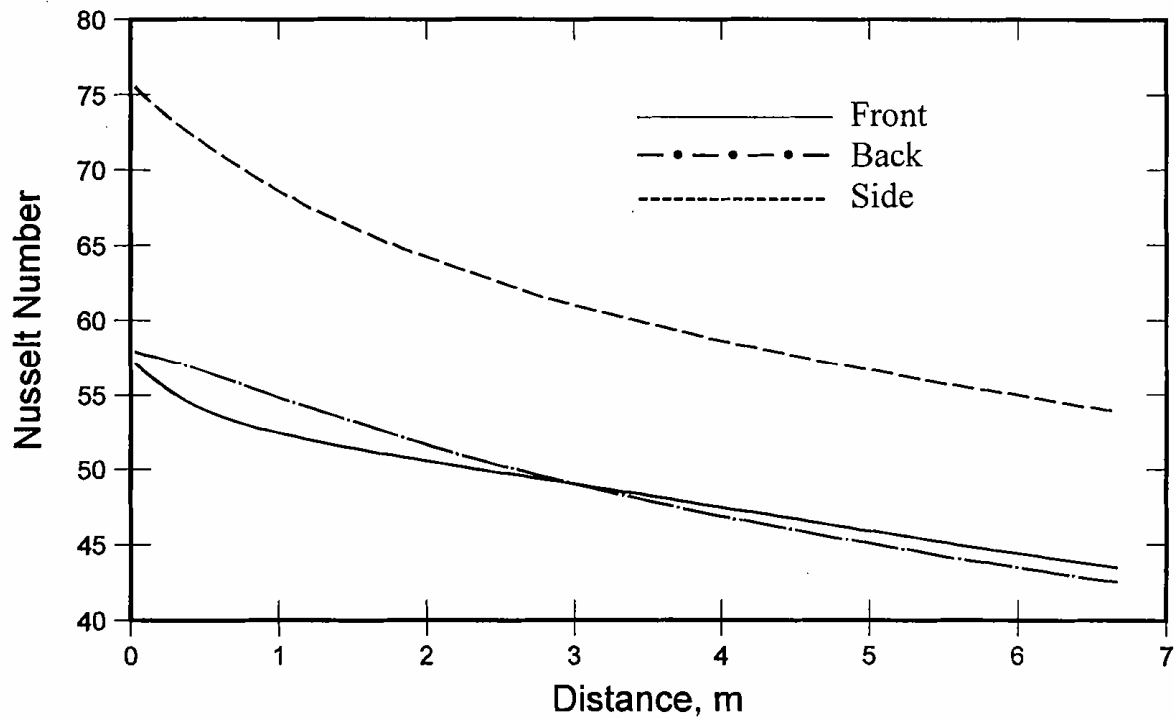

Figure 61. Nusselt number along the axis of the NSTF tube walls (heated wall temperature of 677 °C).
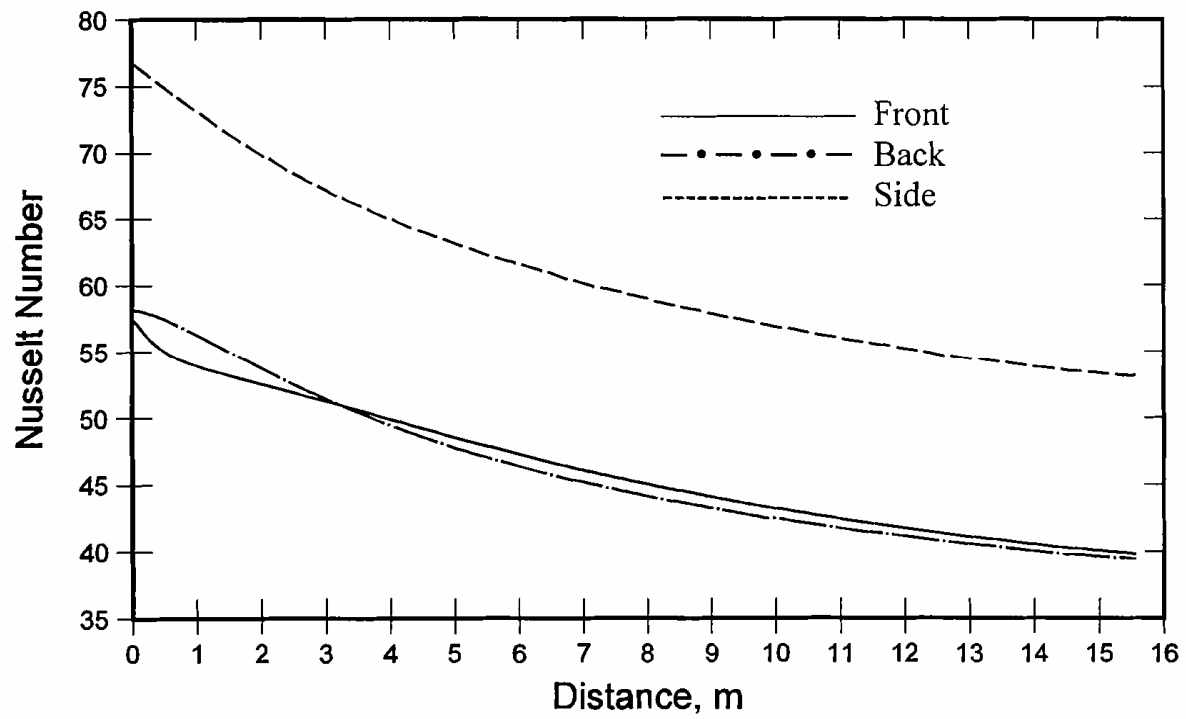
Figure 62. Nusselt number along the axis of the RCCS tube walls (reactor vessel temperature of 560 °C).

Nuclear Engineering Division
Argonne National Laboratory
9700 South Cass Avenue, Bldg. 208
Argonne, IL 60439-4842

www.anl.gov

UChicago ▶
Argonne LLC